INTERFERENCE MANAGEMENT TECHNIQUES FOR FEMTOCELL NETWORKS

A Thesis Submitted to
the Graduate School of Engineering and Sciences of
İzmir Institute of Technology
in Partial Fulfillment of the Requirements for the Degree of

MASTER OF SCIENCE

in Electrical and Electronics Engineering

by
Uğur BAYRAK

March 2015
İZMİR

We approve the thesis of **Uğur BAYRAK**

Examining Committee Members:

Assist. Prof. Dr. Berna ÖZBEK
Department of Electrical and Electronics Engineering, Izmir Institute of Technology

Assoc. Prof. Dr. Barış ATAKAN
Department of Electrical and Electronics Engineering, Izmir Institute of Technology

Assist. Prof. Dr. Özgür TAMER
Department of Electrical and Electronics Engineering, Dokuz Eylül University

13 March 2015

Assist. Prof. Dr. Berna ÖZBEK
Supervisor
Department of Electrical and Electronics Engineering, Izmir Institute of Technology

Prof. Dr. M. Salih DİNLEYİCİ
Head of the Department of
Electrical and Electronics Engineering

Prof. Dr. Bilge KARAÇALI
Dean of the Graduate School of
Engineering and Sciences

ACKNOWLEDGMENTS

I would like to express my sincere gratitute to my advisor Assist. Prof. Dr. Berna ÖZBEK for her guidance, help, understanding and encouragement during the study and preparation of this thesis.

I am thankful to my parents for their supports, understanding and patience through my all education life.

I would like to express gratitudes to Göksenin BOZDAĞ, Deniz PALA, Burçin GÜZEL, Dr. Osman Akın, Dr. İlhan BAŞTÜRK, Basri MUMCU, Bilal Orkan OLCAY, Başak Esin KÖKTÜRK, Tufan BAKIRCIGİL, Şükrü DURBAŞ, Ufuk YÜCEL, Esra AYCAN, Oktay KARAKUŞ and the others for their great supports and friendship.

ABSTRACT

INTERFERENCE MANAGEMENT TECHNIQUES
FOR FEMTOCELL NETWORKS

The need for high capacity and data rate increases with the growing demand for wireless communication. In order to meet this demand, one of the most effective ways of improving capacity and data rate is deployment of femtocell networks which are considered to be a promising technique for future wireless networks. However, mass deployment of these low-power base stations brings many challenges. Interference management will be one of the major challenges for the dense deployment scenarios of femtocells in coverage of the macro base stations. To cope with interference problem, there are many interference management techniques. In this thesis, power control and beamforming techniques are implemented separately and jointly in order to deal with cross-tier downlink interference which occurs between macro base station and users of femtocell. In this two-tier network system involving femtocell and macrocell layers, power control problem, first, is investigated. Feasible transmission power region for femtocell is determined with respect to the user locations so that targeted signal-to-interference-plus-noise-ratio (SINR) values are satisfied. Secondly, beamforming technique is applied using partial zero-forcing method. In this method, beamforming vectors are designed to remove cross-tier interference. It is observed that SINR of macro base station's user does not undergoes any degradation in the nearfield region of femtocell. Finally, we apply these two techniques jointly. Since both interference suppression and power-efficiency is provided, joint technique seems to be a viable and environment-friendly solution for femtocell networks.

ÖZET

EV BAZ İSTASYONU AĞLARI İÇİN GİRİŞİM YÖNETİMİ TEKNİKLERİ

Yüksek kapasite ve veri hızı gereksinimi kablosuz haberleşme için yükselen taleple birlikte artmaktadır. Bu talebi karşılamak için kapasite ve veri hızını geliştirmenin en etkili yollarından biri gelecek nesil kablosuz ağlar için ümit verici bir teknik olacağı düşünülen ev baz istasyonlarının kullanılmasıdır. Bununla beraber bu düşük güçlü baz istasyonlarının yoğun olarak yerleştirilmesi pek çok zorluğu beraberinde getirmektedir. Girişim yönetimi, ev baz istasyonlarının makro baz istasyonlarının kapsama alanlarında yoğun olarak yerleştirilme senaryoları için başlıca zorluklardan biri olacaktır. Girişim sorunuyla başa çıkmak için birçok teknik vardır. Bu tezde, baz istasyonundan kullanıcılara etki eden farklı katmanlar arasındaki girişimi ele almak için güç kontrolü ve hüzmeleme teknikleri ayrı ayrı ve ortaklaşa gerçekleştirilmiştir. Ev baz istasyonu ve makro baz istasyonunu içeren iki katmanlı ağ sisteminde, güç kontrol problemi ilk olarak incelenmiştir. Hedeflenen SINR değerlerinin sağlanması amacıyla ev baz istasyonu için uygulanabilir iletim güç aralığı kullanıcıların konumlarına göre belirlenmiştir. İkinci olarak, hüzmeleme tekniği kısmi ZF metodu kullanılarak uygulanmıştır. Bu yöntemde, katmanlar arası girişimi ortadan kaldırılmak için hüzmeleme ağırlık vektörleri dizayn edilmiştir. Makro baz istasyonu kullanıcısına ait SINR değerinin ev baz istasyonuna yakın alanlarda herhangi bir azalmaya uğramadığı gözlenmektedir. Son olarak, bu iki teknik ortaklaşa uygulanmıştır. Uygulanan bu ortak teknik, hem girişimin yok edilmesi hem de güç verimliliği sağlandığından ev baz istasyonları için uygun ve çevre dostu bir çözüm olarak görünmektedir.

TABLE OF CONTENTS

LIST OF FIGURES

Figure **Page**

LIST OF TABLES

CHAPTER 1

INTRODUCTION

1.1. Overview

The demand for higher capacity and higher data rates increases exponentially. This growing demand in the wireless communication forces researchers to develop new ways of reaching desirable data rates while optimizing cost. With that, a great many of technologies and standards have been developed to overcome this increasing demand. The standards like Long Term Evolution (LTE) and LTE Advanced, 3GPP2s Evolution-Data Optimised (EVDO) and Ultra Wide Band (UWB) and Worldwide Interoperability for Microwave Access (Wimax) have been developed to provide high speed communication to end users [1]. Moreover, to achieve higher capacity, it is necessary for the area of cell to be reduced and for channel reuse to be increased [2].

This demand for cellular services, in fact, originates from indoor with the gradually-increasing use of mobile devices such as smart phones etc. in recent years. In accordance with the recent surveys, 50 percent of phone calls and 70 percent of data services will take place indoors in the next years [3]. That is why it is important for cellular networks to provide good quality coverage to indoor users. Furthermore, with the years passing, the new multimedia services and high data rate applications make the indoor coverage quality one of the upmost issues in terms of the service providers. To provide good quality indoor voice and data services is of great importance to the cellular operators in respect of increased revenue and reduced churn as well.

Macro Base Stations (MBS) have some kind of drawbacks when it comes to indoor communication. There is no denying fact that they have huge coverage and power to satisfy users. But drawbacks such as propagation loss, penetration loss etc. impose a burden on MBSs to provide good quality of service to the indoor users. Due to the penetration loss, the indoor user requires high power from the serving MBS, which leads other users to have less power and with the result that the overall system throughput reduces. To meet the needs of high capacity network, having a great number

of MBSs is also expensive. In terms of network planning and optimisation, the large number of MBSs would pose a larger burden [4].

This situation lays emphasis on having indoor coverage solutions. One of these solutions is picocells. Picocells are small cells, providing coverage for indoor environments. These can be located to large buildings, hot spots such as airports, universities, shopping malls. Picocells work the same way as macrocells and are connected to one another through cables or radio links [5]. The other solution for the indoor coverage problem is Distributed Antenna Systems (DAS). This system consists of a number of distributed antenna elements and a home base station. The antenna element are connected to the home base station through dedicated cables or RF links. With that, this makes it possible to provide good quality of service for indoor environments where MBS can not reach. Even though picocells and DAS provide good and cost-efficient solution compared to the outdoor macrocell, these are still too expensive to be deployed for indoor users. And also, to install these systems in every building and residence would cost too much [6].

One more indoor coverage solution, expected to be one of the most-promising technologies in the future, is Femtocells. Femtocells, also known as home base station, are small, low power access points and visually look like an ordinary wireless router [1]. These access points, known as Femtocell Access Point (FAP), create small wireless coverage area and connect user equipment to the cellular core network through the subscriber broadband internet access. Owing to the fact that these are installed by the users, it is cost effective solution as compared to other indoor coverage solutions.

Femtocells are of great use to both indoor users and operators. Users can experience better signal quality in indoor environments with the use of these devices. Femtocells also provide power savings, reduced energy consumption. Moreover, since user equipment (UE) such as mobile phone does not need to communicate with the MBS which is far from the UE, femtocells lengthen the battery life of the UEs [2].

Compared to the aforementioned small cell concepts, femtocells provide better indoor coverage solution. However, they are faced with many challenges at the same time [7]. One of the most important challenges of femtocell is interference management since femtocells are greatly likely to be deployed so densely in the future. Also, because of the ad hoc nature of femtocells, they are in need of some intelligent techniques to organize themselves in order to cope with the interference problem. For this reason, interference management techniques are of great importance for femtocell network to

ensure that users have good quality of service without any degradation effect in system parameters such as signal-to-interference-plus-noise ratio (SINR).

In this thesis, in order to improve the system performance, interference management techniques are dealt with. Power control and beamforming techniques are separately implemented in single and multiple FAP environments, respectively. Then, the joint power control and beamforming technique is proposed in both single and multiple FAP scenarios.

1.2. Thesis Outline

Chapter 2 is devoted to the background information for wireless channels and femtocell. Multiple antenna concept and capacity are given. Some parameters of path loss model used in thesis work are shown. Femtocell concept is explained in detail.

Chapter 3 deals with the power control technique. This technique, after overviewed, is formulized and simulation results are examined. It is applied separately for both single FAP and multiple FAPs cases. Also, the network system models to be used in the whole thesis work are illustrated in this chapter.

Chapter 4 is concerned with the beamforming technique. First, a brief information is given on the matter. Then, in single FAP case, sytem model is explained and simulation results depending on the this system model are illustrated. Finally, the beamforming technique in multiple FAPs is treated in this chapter. In here, system model is shown and simulation results are evaluated.

Chapter 5 proposes the joint power control and beamforming technique in single FAP and multiple FAPs cases, respectively. The algorithm is given in detail and then the simulation results of this technique is shown.

In Chapter 6, conclusion of the thesis is presented and future works are given.

CHAPTER 2

BACKGROUND

2.1. Wireless Channels

Wireless channel is the medium in which transmitted signals propagate to the receiver. In wireless communication, signal radiated from transmitter antenna propagate through one of three routes: ground wave, sky wave or line of sight propagation [8]. Each of these routes is formed of due to the fact that signals with different frequencies have different propagation characteristics.

The wireless channel poses a lot of challenges, making it difficult for reliable communication to be achieved. It contains many parameters like mountains, hills, houses, moving users or another objects. Some of the parameters change over time in unpredictable way and this unpredictable nature of the wireless channel poses a large burden on reliable high-speed communication as well. Multipath and shadowing effect, Doppler shift, time dispersion and delay spread account for that nature of the wireless channel.

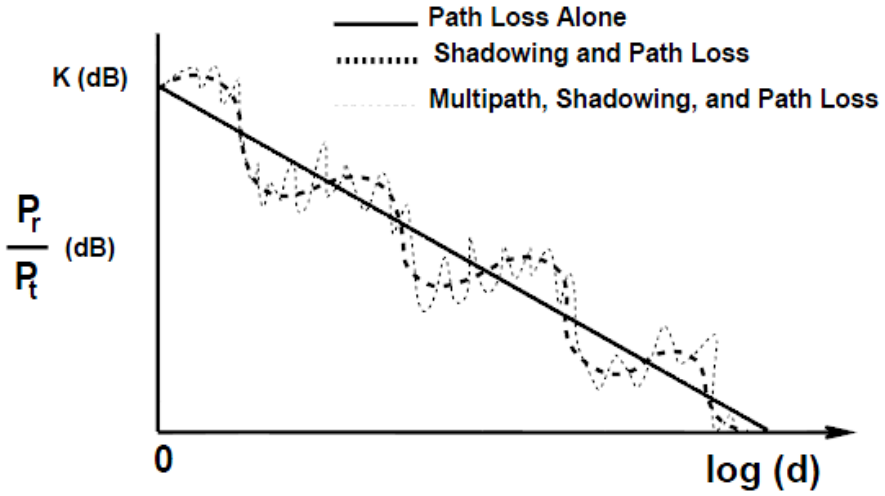

Figure 2.1. Path loss, Shadowing and Multipath versus distance
(Source: Goldsmith, 2005)

In terms of fading characteristics of the wireless channel, there are two types of fading, named as large-scale fading and small-scale fading. Large-scale fading is the signal variations or attenuations over large distances. Path loss and shadowing effects fall into this category. Small-scale fading is due to the constructive and destructive effects of multiple signals over a short distance or short period of time. Multipath effect can be counted in this fading category [9]. Path loss, shadowing and multipath effect with respect to logarithmic distance are illustrated in Figure 2.1.

2.1.1. Path Loss and Shadowing

Path loss results from dissipation of the transmit power of signal comparatively to the propagation channel distance. As far as free space path loss is concerned, there are no obstructions between transmitter and receiver and consider a transmitter is located at distance d from receiver. This link has a line of sight (LOS) propagation.

The transmitted and received power is P_t and P_r, respectively, so the ratio of received to transmitted power is

$$\frac{P_r}{P_t} = \left(\frac{\sqrt{G}\lambda}{4\pi d} \right)^2 \tag{2.1}$$

where G is antenna gain factor, d is the distance between transmitter and receiver and λ is the signal wavelength [9].

As seen, the received power decreases inversely proportional to the square of the distance d between transmitter and receiver. Also, the received power is proportional to the square of the signal wavelength. Thus, the carrier frequency and received power is inversely proportional. The abovementioned expression can be written in dBm so that link budget can be calculated effectively. The received power in dBm is expressed by

$$P_r\ dBm = P_t\ dBm + 10\log_{10}(G) + 20\log_{10}(\lambda) - 20\log_{10}(4\pi) - 20\log_{10}(d) \tag{2.2}$$

Free space path loss is defined as

$$P_L\ dB = 10\log_{10}\frac{P_t}{P_r} = -10\log_{10}\left(\frac{\sqrt{G}\lambda}{4\pi d}\right)^2 \tag{2.3}$$

Furthermore, there is a simplified model for path loss in order to describe and find an aproximate value. In this model, reference distance d_0 and path loss exponent are chosen depending upon propagation environment. So, the mean path loss is defined as [9]

$$\overline{PL}(d) = \left(\frac{d}{d_0}\right)^n \tag{2.4}$$

The mean path loss is often expressed in decibels

$$\overline{PL}(d) = \overline{PL}(d_0) + 10n\log_{10}\left(\frac{d}{d_0}\right)\ (dB) \tag{2.5}$$

where n denotes path loss exponent which means the rate at which path loss increases with distance. The value of n depends on the propagation environment. In free space, for example, n is equal to 2. In case of obstructive environment, the value of the path loss exponent n will be stepped up correspondingly.

It is important that a free space reference distance is appropriately selected for the specific propagation environment. In large coverage cellular systems (Macrocells), reference distance (d_0) with 1000 meter is chosen in general, while, in small coverage cellular systems (Microcells), 100 meter or 10 meter can be used. In addition, 10 meter is generally preferred for indoor cells such as femtocells. The reference path loss is determined either using free space path loss formula which is given by Equation (2.3) or using field measurements at a distance of d_0 [9].

For macrocell path loss effect, the following is used [10].

$$\mathrm{PL(outdoor)} = 128.1 + 37.6\log(d \quad [\mathrm{km}]) \tag{2.6}$$

To characterize the femtocell path loss effect, indoor propagation of IMT-2000 model is used [10].

$$\mathrm{PL(indoor)} = 37 + 18.3 + 30\log(d \quad [\mathrm{m}]) \tag{2.7}$$

By using these two path loss model, obtained results for macrocell and femtocell are illustrated in Figure 2.2 and 2.3, respectively.

A signal transmitted through a wireless channel also experiences random variation due to blockage from objects in the signal path, giving rise to random variations of the received power at a given distance. Such variations are also caused by changes in reflecting surfaces and scattering objects. Thus, a model for the random attenuation due to these effects is needed. Since the location, size and dielectric properties of the blocking objects as well as the changes in reflecting surfaces and scattering objects that cause the random attenuation are generally unknown, statistical models must be used to characterize this attenuation. The most common model for this additional attenuation is log-normal shadowing [9].

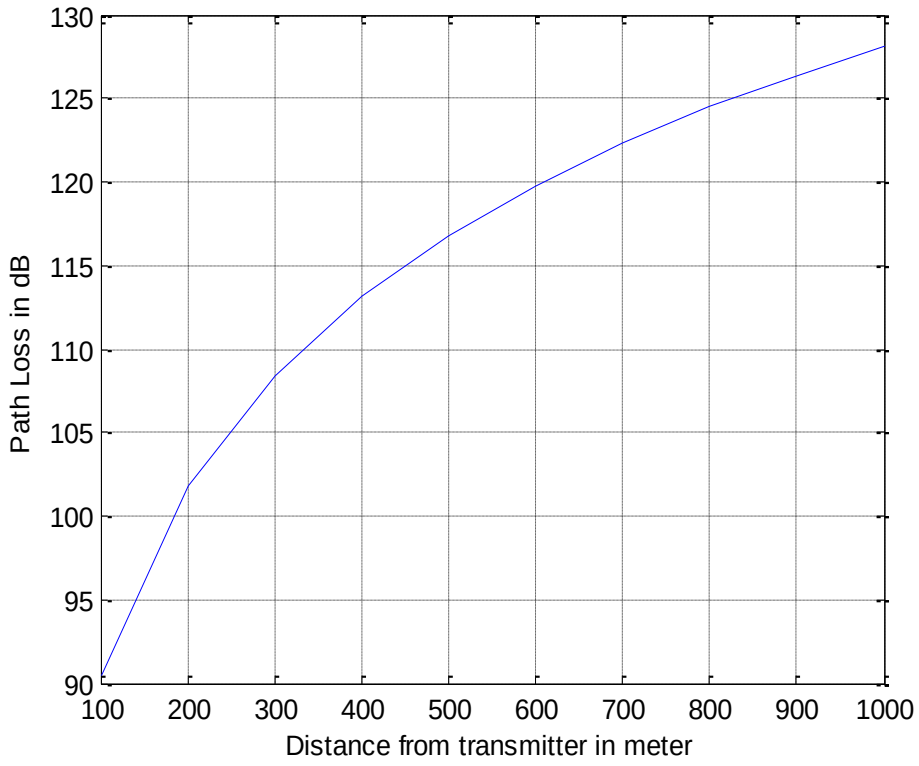

Figure 2.2. Macrocell outdoor-path loss versus distance

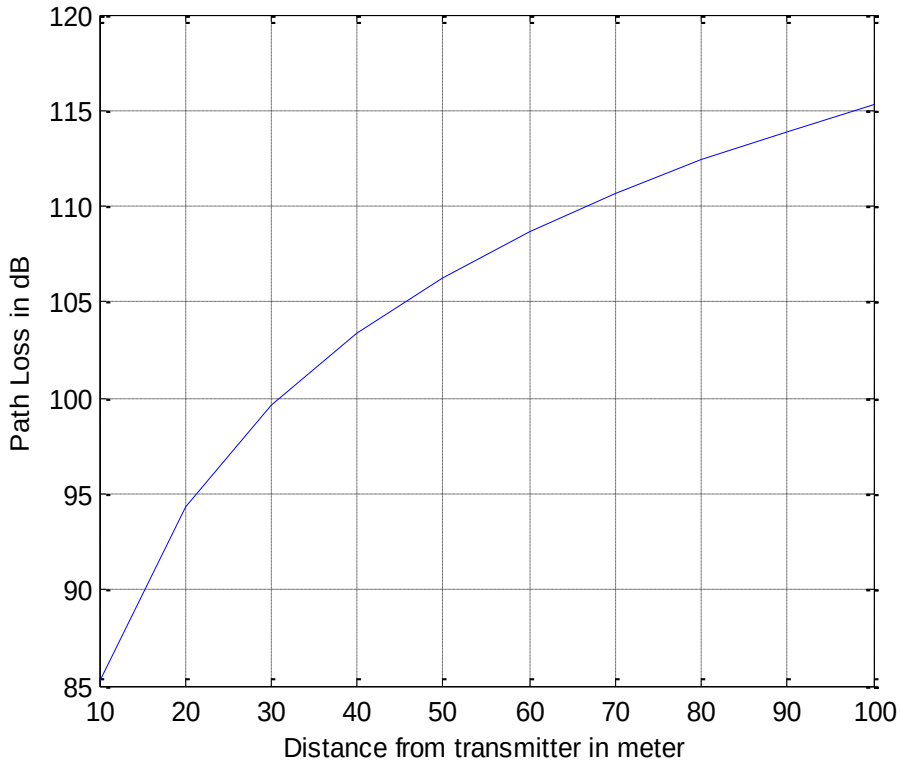

Figure 2.3. Femtocell indoor-path loss versus distance

2.1.2. Multipath effect

In a wireless channel, transmitted signal can travel to receiver through multiple paths, with the result that, each part of the transmitted signal which travels along different paths arrives at receiver point at different times. This phenomenon is called multipath propagation. Because of this phenomenon, received signal can vary widely in amplitude and phase. Multipath propagation is constituted of three phenomena. These are reflection, diffraction and scattering.

Reflection occurs when electromagnetic wave bounces off an object including buildings, walls and so forth. Due to this objects, there is no single line-of-sight path to the base station. Additionaly, even, in the absence of any object along the path, multipath still occurs due to the reflections from the ground surface.

Diffraction is caused by the fact that transmitted signal is blocked by an object with sharp irregularities. With that, diffracted signal can propagate behind the obstruction. Scattering results from the fact that electromagnetic wave strikes object which its dimension are small compared to the wavelength. Therefore, the reflected

signal is spread out in all directions when it hits on a rough surface. As a consequence, all of these phenomena cause not only dissipation of the signal energy but also intersymbol interference. In this work, multipath effect is modelled using Rayleigh fading model [9].

2.1.3. Noise

It is important for wireless systems to provide a certain minimum transmission quality. Transmission quality is related to the Signal-to-Noise Ratio (SNR) at the receiver as well. System reliability or , in other words, minimum transmission quality is determined by a certain threshold SNR value.

In order to find this SNR value in system modelling, thermal noise is used. First, noise power spectral density is [9]

$$N_0 = k_B T_e \tag{2.8}$$

where k_B is Boltzmann's constant, $k_B = 1.38 \,.\, 10^{-23}\ J/K$, T_e is 300K around which the temperature of the Earth is. In an additive white Gaussian noise (AWGN) channel, the noise is a white Gaussian random process with mean zero and power spectral density $N_0/2$. Since the noise has uniform power spectral density $N_0/2$, the total noise power within the bandwidth 2B is [9]

$$P_n = (N_0/2) \times (2B) = N_0 B \tag{2.9}$$

where B is bandwidth in Hz.

2.1.4. Capacity of wireless channel

According to the Shannon, reliable communication can be achieved at strictly positive data rate but at the same time with as small error proability as desired with the help of intelligent coding of the information. However, there is a maximum data rate for

given channel to communicate reliably, which is called capacity. This is such maximal data rate that if one attempts to communicate at a rate above the channel capacity, it is impossible for error probability to reduce to zero.

To illustrate the general formula of capacity, in the event that there is only one base station, the equation shown below can be written [9].

$$\mathrm{C} = B\, \boldsymbol{E}\left[\log_2(1+\frac{P_r}{\mathrm{N}_0 B}) \right] \tag{2.10}$$

where B is the bandwidth and N_0 is the noise power spectral density of AWGN channel. P_r is the received power and its formulation is as follows.

$$P_r = \frac{P_t}{PL}\left|h\right|^2 \tag{2.11}$$

where P_t is transmission power of base station and h is channel coefficient including multipath effect. PL represents path loss and shadowing effects.

In the event that there are two base stations, the general capacity formula is written as follows.

$$\mathrm{C} = B\, \boldsymbol{E}\left[\log_2(1+\frac{P_r}{P_I + \mathrm{N}_0 B}) \right] \tag{2.12}$$

where P_r is received power. P_I is interference power from the other base station. The formulation these powers are as follows.

$$P_r = \frac{P_{t1}}{PL_1}\left|h_1\right|^2 \tag{2.13}$$

$$P_I = \frac{P_{t2}}{PL_2}\left|h_2\right|^2 \tag{2.14}$$

2.1.4.1. Capacity Improvement with Femtocells

Femtocells make it possible to increase the mobile users per area. This means that capacity per area can be enhanced by deploying femtocells at the places where macrocell is insufficient to provide needed data rate. In the following pages, data rate improvement with femtocells is illustrated in the process and the scope of thesis work.

In these figures, macrocell is located at the origin. Figure 2.4 illustrates the capacity distrubution of macro base station along the coverage area in meter according to Equation (2.10). In Figure 2.5, there are one macro base station at the origin and a few femtocells located at different places. This figure represents total capacity distribution with no interference since it is assumed that spectrum of femtocell and macrocell is equally divided. It clearly shows to what extent the capacity per area can be enhanced deploying femtocells.

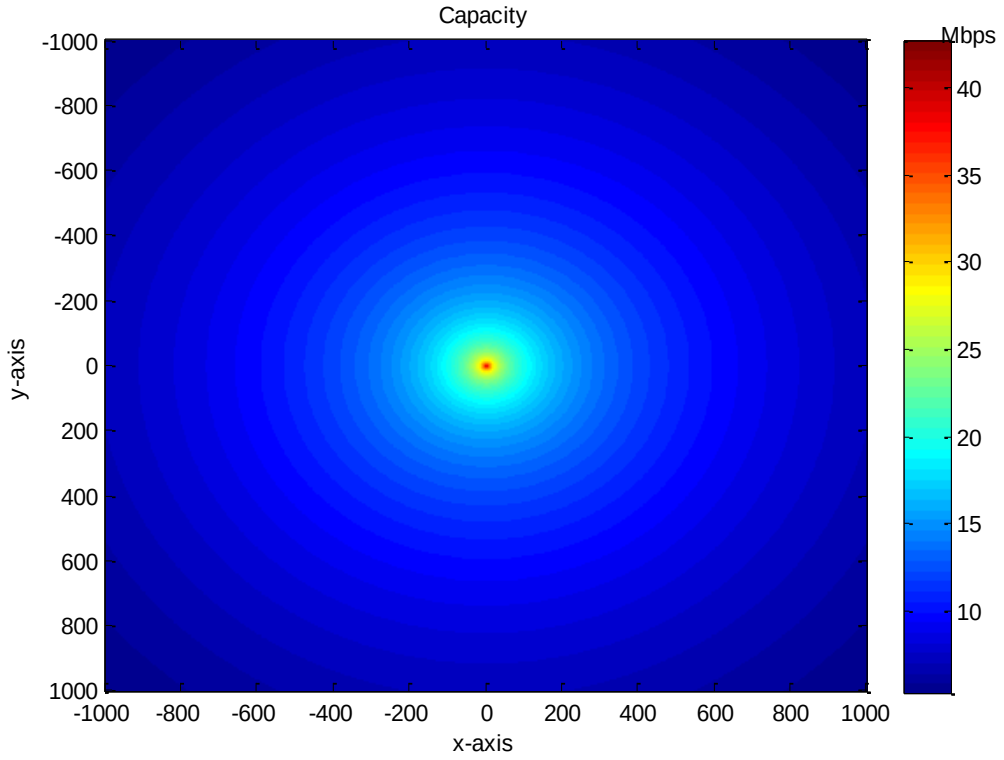

Figure 2.4. Capacity distribution of macro base station coverage area [m]

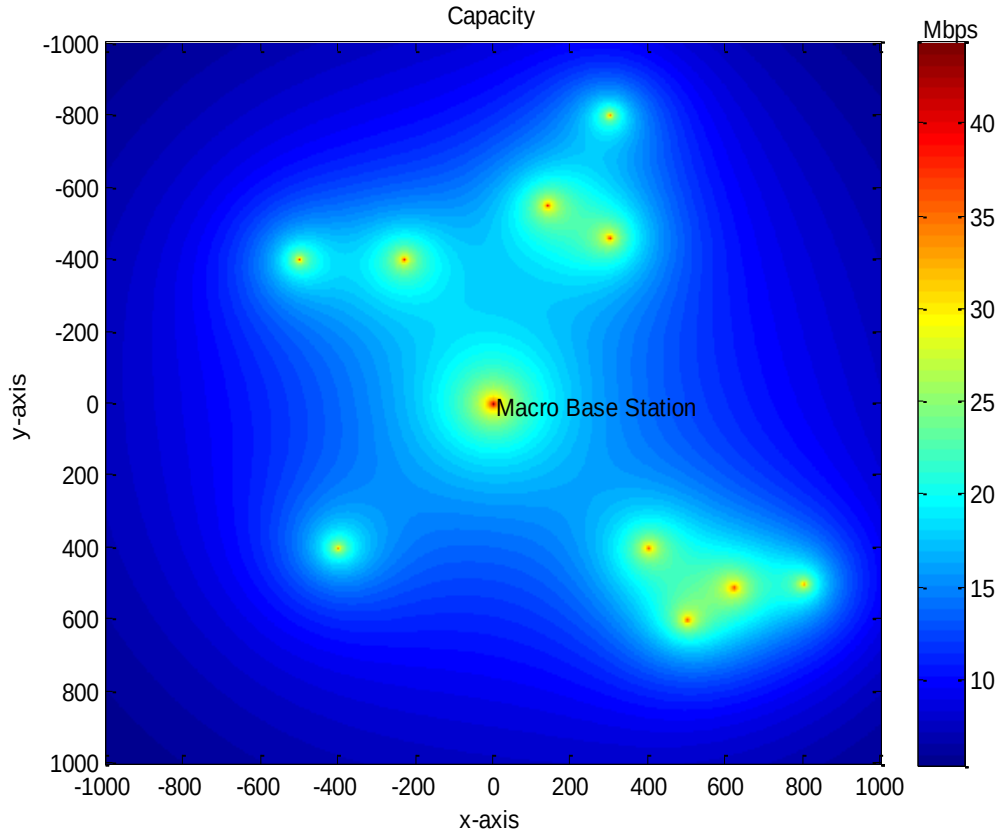

Figure 2.5. Total capacity distribution of both macrocell and femtocells

2.1.5. MISO (Multiple Input Single Output) Wireless System

2.1.5.1. Overview of Multiple Antenna Concept

Over the last 20 years, multiple antenna techniques have been regarded as a key technology to enhance communications through a wireless channel. Even though the first beamforming concepts date back 50 years, it is only since the mid-1990s that multiple antenna techniques has been attracting a great attention in the research community first and then in industry [11].

Multiple antenna techniques consist of MIMO (multiple-input multiple-output), MISO (multiple-input single-output) and SIMO (single-input multiple output) systems, and they can be categorized into spatial diversity, beamforming and spatial multiplexing techniques. These are summarized with their benefits in the following figure.

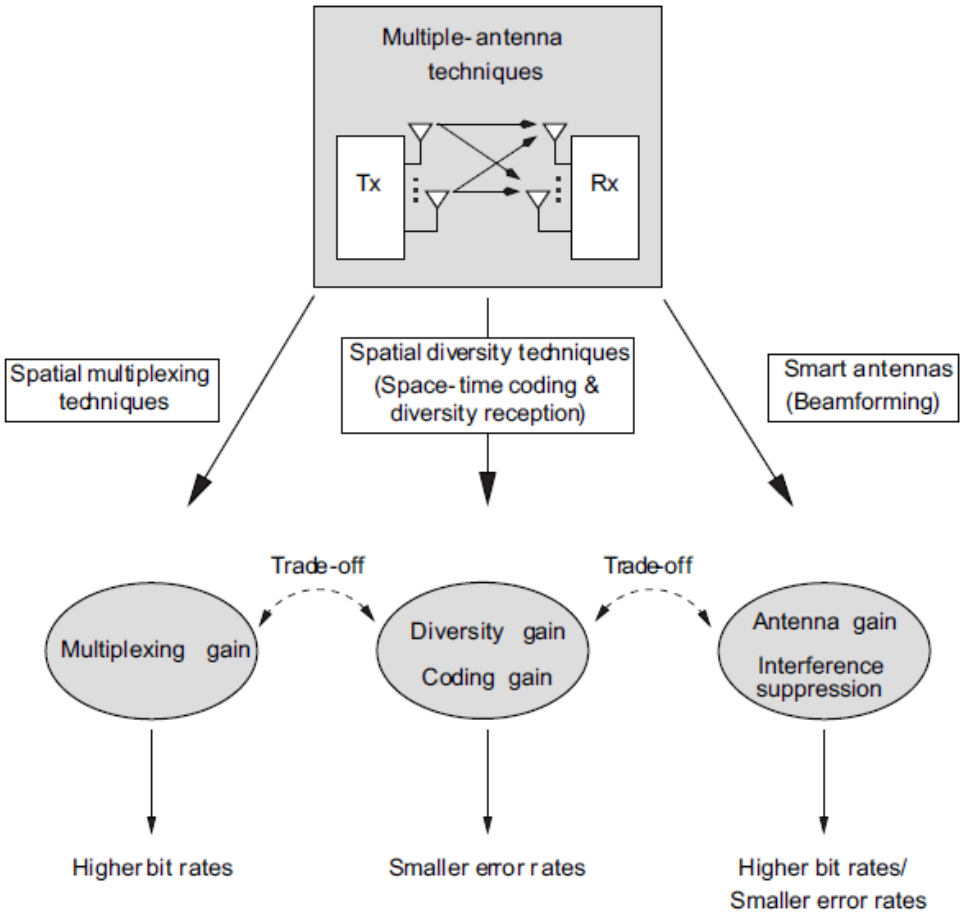

Figure 2.6. Summary of multiple antenna techniques [11]

Spatial multiplexing techniques make it possible to simultaneously transmit independent information sequences, which is called layers, over multiple antennas. In other words, multiple data layers are send in parallel through different spatial dimensions. Thus, the overall bit rate when compared to a single antenna system is increased by a factor of the number of antenna used without requiring extra bandwidth or extra tranmission power. Channel coding is often used to provide a certain error performance.

By transmitting or receiving the same information sequence over different antennas, spatial diversity techniques provide smaller error rates. By means of two dimensional coding in time and space, commonly referred to as space-time coding, the information sequence is spread out over multiple transmit antennas. At the receiver, an appropriate combining of the redundant signals has to be performed. Optionally, multiple receive antennas can be used in order to improve the error performance (diversity reception).

In addition to these two technique, beamforming, as the name suggests, is a technique in which antenna beams are able to be formed by means of smart antennas, also called adaptive antennas, toward desired areas. In this way, using beamforming technique, beam patterns can be guided to the certain desired directions and SINR values at the receiver can be improved to a large degree. Actually, beamforming is an array processing technique. Comprehensive researches on smart antennas for wireless communication systems just started in 1990s [11].

2.1.5.2. Capacity of MISO channels

A MISO channel $(N_t \geq 2, \mathrm{N_r} = 1)$ has channel vector **h** = $[h_{11}\, h_{12} \ldots.\ h_{1N_t}]^t$ with the size of $N_t \times 1$. The gain is given as

$$\lambda = \|\boldsymbol{h}\|^2 = \sum_{j=1}^{N_t} \left| h_{1j} \right|^2 \tag{2.15}$$

And then capacity formula of MISO channel is obtained as follows [9].

$$C_{MISO} = B\, \boldsymbol{E}\left[\log_2 \left(1 + \frac{P_r}{N_t N_0 B} \right) \right] \tag{2.16}$$

where P_r is the received power and N_t is the number of transmit antennas. Formulation of the received power is as follows.

$$P_r = \frac{P_t}{PL} \|\boldsymbol{h}\|^2 \tag{2.17}$$

where P_t is transmission power of the base station and $\boldsymbol{h}$ is channel vector including multipath effect. PL represents path loss and shadowing effects.

2.2. Femtocells

2.2.1. Description of Femtocell Concept

The concept of femtocells date back to the 1999, when Bells Labs first studied a home base station. The Alcatel announced that a GSM based home base station would be come on the market in 2000. Afterwards, in 2002, Motorola announced 3G home base station but the concept was still very new. This concept became more famous in 2005 and came to be called " Femtocell " in 2006. A number of companies released trials and demonstrations [12].

Femtocells are low-power home base stations which provide radio coverage to the mobile users in an indoor environment [1]. These devices are installed by the end user and bring a solution to the operator's installation expenditures. Femtocell is connected to the core network through the broadband internet connection [7]. The connection from end user to the operator's core network is shown in Figure 2.7.

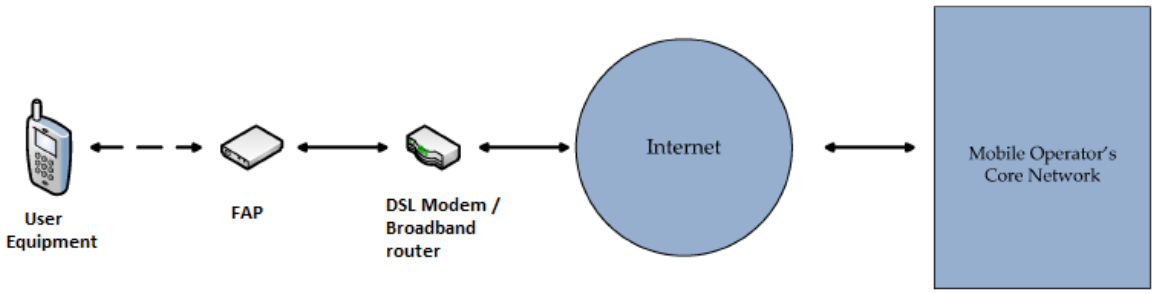

Figure 2.7. Femtocell connection from UE to operator's core network

Thus, data and voice services can reach to the indoor users by FAPs. Femtocells use the same physical layer technology as cellular networks, which are referred to as Home Node Bs (HNB) in WCDMA systems and are referred to as Home evolved Node Bs (HeNB) in LTE systems [7].

Femtocells have ad hoc topology and any user can deploy in its home and even can move femtocell from one place to another. It is because femtocells have these features that they are faced with many challenging problems.

2.2.2. Technical and Business Aspects of Femtocells

2.2.2.1. Technical Aspects

Femtocells have a small cell radius due to their low power, so that the distance between transmitter and receiver is reduced. Thus, the signal from transmitter is less attenuated, which enable femtocells to have better signal quality. Strictly speaking, femtocells can provide a better solution for the indoor environment. In addition to that, due to their low transmit power, femtocells make use of indoor walls as an insulation by means of penetration losses of walls while maintaining good coverage quality. As a result, good channel conditions make it possible for femtocells to provide high data rate services like 3G [7]. Moreover, a femtocell usually serves a very small number of user in contrast to the macrocell. It should come as no surprise that this property enables them to provide good quality of service (QoS) to users when compared to the macrocells which have to serve great number of users in a larger area [13].

In respect of spectrum utilisation, femtocell has two main modes of deployment: the separate channel deployment and the co channel deployment [14]. In separate channel deployment, femtocell allocates the specific channel which is not used by macrocell. Given that spectrum allocation, interference problem are avoided. In the co channel deployment, femtocell share the same portion of spectrum with macrocell. Using the same spectrum rather than dedicating it is much favoured by operators because spectrum is so expensive that excessive amount of use of spectrum costs too much. The co channel deployment also increases the overall system capacity. But interference problem must be taken into account as well. For this reason, intelligent and efficient interference management techniques are required.

2.2.2.1.1. Types of Femtocells

Given various air interface technologies, femtocells have been categorized into different types with related to these technologies. Being compatible with every kind of technologies, femtocells provide different types of service. The main types of femtocells are shown in Figure 2.8.

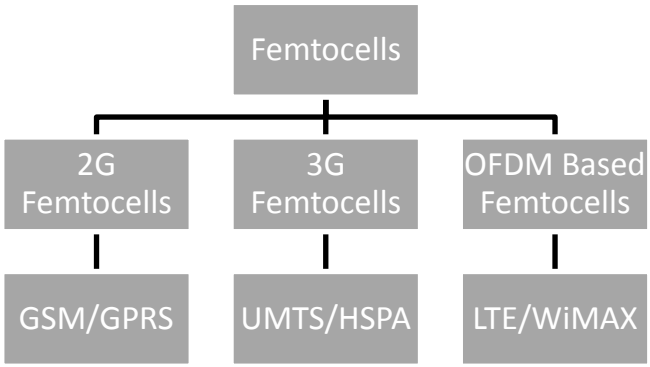

Figure 2.8. Types of Femtocells

2G Femtocells are based on the Global System for Mobile Communication (GSM) air interfaces. GSM holds a great number of subscribers around the world. Especially in developing countries like India and Pakistan, GSM is still spreading [15]. One of the main reasons of development of 2G femtocells is its low cost.

The development of 2G femtocell did not stand on its own feet because of its drawbacks. The main disadvantage is that GSM femtocells use General Packet Radio Service (GPRS) for data services, which does not support high data rates. Hence its use is only limited to the good quality voice. In parallel to that situation, it is quite normal for GSM femtocells to be mostly used in developing countries where cellular networks are only used for voice services [16].

3G Femtocells are based on the air interface of Universal Mobile Telecommunication System (UMTS) [17]. These femtocell can provide higher data rates as compared to the 2G femtocell. The UMTS technology is capable of connecting through IP based networks, which attracts great attention manufacturers. The UMTS femtocells are also standardised by 3GPP as HNBs [18].

As for OFDM based femtocells, the WiMAX and LTE femtocells come under this category [19]-[20]. LTE femtocells can provide high data rates. These femtocells can be considered as a promising indoor technology.

2.2.2.1.2. Access Modes of Femtocells

Femtocells are generally designed to be able to operate in three different access modes: Open Access Mode, Close Access Mode and Hybrid Access Mode. These modes determine which user is supported by so-called femtocell [21].

In the open access mode, all users in coverage area user can access the femtocell and benefit from its service. This access mode usually improves indoor capacity to a large extent. Home user as the owner paying for service is unlikely to use open access mode because every user can access and user does not share its service with any other else. Open access mode can be used mostly in public areas like airports, hospital, shopping malls and makes a great contribution to the capacity of that areas.

In the closed access mode, the femtocell allows only subscribed users to connect. Home users generally prefer closed access mode so as to make use of their own service. However, unsubscribed users cause interference. Users in closed access can experience high level signals from unsubscribed ones, most of which causes users not to be able to establish a connection with the femtocell.

In the hybrid access modes, it is allowed the connectivity of nonsubscribers while giving priority to the subscribed used. By means of this mode, abovementioned interference problem in closed access mode can be eliminated by controlling the users giving rise to interference signal.

2.2.2.2. Business Aspects

Within the last decade, femtocells have blazed a new trail in communication world and taken a huge step further and attracted a great attention in terms of the business perspective. A large number of service providers have come to become interested in using, deploying and marketing these devices in the respect that femtocells offer them to increase their revenue and boost network capacity. Therefore, by making an invesment in femtocells, they can make a considerable profit.

Yet, macrocell with high-priced infrastructure, operational expenditure (OPEX) and capital expenditure (CAPEX) does not seem to be viable solution at a time when data and voice traffic growth reach to a maximum and dense deployment is required. When compared to the macrocell, femtocells have a great advantages when it comes to

the economic issues. The most important economic aspect is that they are user-deployed devices, which leads operators to make the most of their revenues as much as they can. In other words, this results in reducing OPEX and CAPEX to a large degree. Operators not only maximise their revenue but also increase networks capacity with help of small cells. As a result, femtocells provide a cost-effective solution for the overall network cost [22].

Keeping benefits in mind, manufacturers are still concerned about the price and services of femtocell which is in competition with Wi-Fi [23]. For this reason, femtocells ought to offer legitimate solutions and prices compared to the Wi-Fi in order to continue its existence in the years to come. It is normal for manufacturers to have doubts about femtocells because they are new-integrated devices for communication industry and also they have some drawbacks. One of the main drawback is that femtocell users must have broadband internet connection in their residences. Femtocell depends on the backhaul connection. Any failure in the internet connection gives rise to failure in femtocell.

In contrast to these drawbacks, by having cognitive capabilities and opportunistic spectrum access, femtocells provide more viable solution from the business point of view to all intents and purposes. They enable operators to use spectrum in more efficient way. With the self organizing nature, femtocells make it more possible for operators to cope with network planning and optimisation.

2.2.3. Technical Challenges in Femtocells

Much as femtocells are of great use to many respect of network coverage and capacity, they have, of course, challenges and disadvantages when it comes to dense deployment scenario in urban areas especially. Determining what kind of challenge will be dealt with and to what extent it is known by those involved in the matter is of crucial importance for femtocells to work in a seamless and robust way.

2.2.3.1. Mobility Management and Handovers

Coverage area of femtocell is small, so that it is quite necessary to control and support handovers in order to provide users with continuous connection. Because of

small coverage, the number of users in femtocell coverage area can rapidly change in a very short time. Especially in dense-deployed environments, user traffic reaches a huge numbers. That being the case, mobility management and handover procedures would be required. In the event that femtocell is surrounded by a large number of neighbours, it is very difficult for femtocell to keep track of its users which continually get around between femtocell coverage layers. Furthermore, access modes being used largely affect handovers. Open access mode paves the way for a large number of handovers while other modes reduce [7].

2.2.3.2. Self Organisation

Since femtocells are user-deployed devices, they can be switched on or off at any time and they can be moved to anywhere. These event occurs randomly and the number of femtocell in a location is completely unpredictable. Taking all of these into consideration, it makes classic network planning and optimisation impossible. Femtocells are in need of a new optimisation and planning method. The most promising solution for femtocell is to integrate itself autonomously into the access network. To that end, they need to have self configuring capabilities [24]. This kind of capability helps femtocell configure and optimise itself without posing any burden on the network and in this way, improves its performance in terms of capacity. Also, by removing human involvement, operational expenditure is reduced to a large extent.

In the event that femtocell is moved to another location, femtocell need to self-configure in order to adopt and establish a connection with different cell sites without any human involvement. This is an important property in terms of future wireless networks. To have such capabilities enable femtocell to sense its environment and configure its parameters with respect to the continually-changing settings [25].

In case of dense deployment, most likely to take place in future networks, femtocells have to be able to adjust its network parameters to acceptable levels with the help of self optimising in order to operate successfully. Self optimisation is concerned with many parameters such as transmission power, access modes, pilot power, handover control and sensing etc. Recent years, many researches have been done in this area and as the time goes on, the problem of self organising is greatly likely to become more challenging.

2.2.3.3. Timing and Synchronisation

There is no centralised network management of femtocells because of their user-deployed nature [21]. However, in a wireless system, it is excessively needed for devices to be synchronised by central network in order not to cause any Inter Symbol Interference (ISI), which leads to a large amount of signal degradation and unreliable data communication. Without timing, transmission instants can also vary among different cells. For this purpose, good quality oscillators can be used in FAPs but they are so expensive and considering dense deployment scheme including many FAP, these oscillators would increase the overall cost.

Keeping in mind that FAPs are connected to the core network through Asymmetric Digital Subscriber Line (ADSL), syncronisation can be provided by using that line. FAPs use the ADSL to take clock-timing of the operator core network and thus, reliable and sychronised data communication can be achieved. However, the acquired signal timing may contain some unpredictable delays [7].

One another solution can be using the GPS [7]. The GPS module within the femtocell provides a clock-timing by received the GPS signal. This can also be used for the purpose that femtocell users are able to reach to local news and information. However, the GPS signal much more attenuates when it comes to indoor environments. As seen, many techniques at hand have been applied to deal with timing and synchronisation problem up to now. And, intelligent techniques and algorithms are needed to be developed at full length.

2.2.3.4. Interference

Given a mass deployment of femtocells, interference problem is greatly likely to be ranked first and have a huge impact on femtocell operation and network designing. Aiming at reducing cost and improving capacity, the operators prefer co-channel deployment, so that this use of the same portion of spectrum gives rise to interference [7]. It might seem reasonable to use separate portion of spectrum for macrocell and femtocell, respectively, on the other hand, spectrum costs too much and this is not good for operators.

Interference causes a strong degradation of both femtocell and macrocell user's performance. Each new deployed femtocell can disturb each other's normal functioning. Considering two-tier networks, interference signals cause "dead zones" in other existing layer of network [21]. Dead zones can occur in both femtocell and macrocell coverage area due to the strong interfering signal. Therefore, various interference management techniques such as interference avoidance and cancellation has been developed to that end.

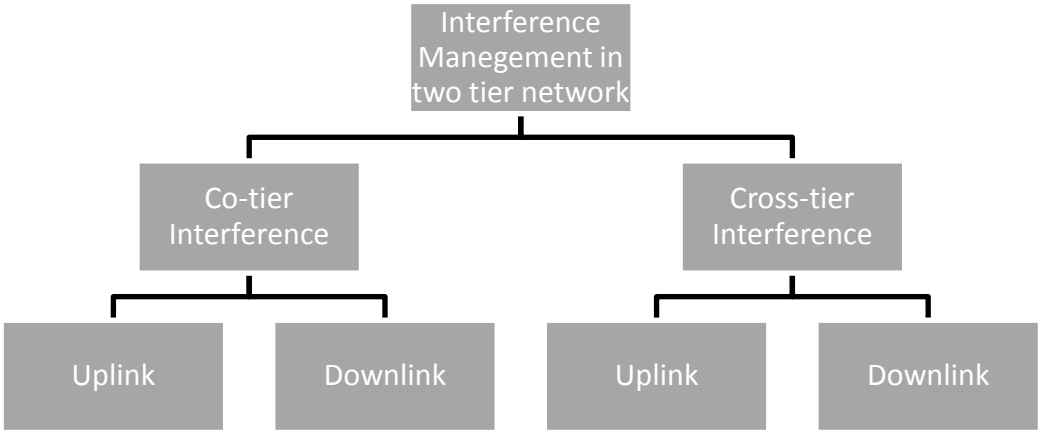

Figure 2.9. Types of interference management in two-tier network

There are great deal of interference avoidance techniques for femtocell networks. First, spectrum splitting can be suggested [26]-[27]. In this technique, spectrum band is divided into two portions. One portion is allocated for macrocell while the other one is allocated for femtocell. However, this is not a cost-efficient technique due to scarcity of spectrum and high cost. In some cases where dense deployment of femtocell is concerned, separate portion of spectrum can be used for femtocell operations [28]. Power control is also a key technique in the interference avoidance. In this technique, by controlling the transmit power of femtocell, macro user in the vicinity of the femtocell can be protected. Recently, this technique is carried out by using game theory. One such technique is proposed in [29], where macro and femto base stations operate in semi-autonomous mode in order to maximize energy-efficiency. Each base station updates its power allocation strategy to maximize its utility. Another power control technique is based on Stackelberg game. In these proposed techniques [30]-[31],

macro base station acts a leader while femtocells act as a followers. Leader adjusts its power and imposes interference price on followers to maintain its user's minimum rate requirements. Subsequently, followers optimize their powers based on the imposed price. The similar technique used in [32]. In order to achieve much more effective interference management technique, cognitive capabilities of femtocells can be used for interference mitigation [33].

2.2.3.4.1. Co-tier Interference

This type of interference occurs among the networks elements belonging to the same tier of the network. Co-tier interference is illustrated in Figure 2.10 with respect to femtocell layers. In dense deployed femtocell environments, femtocell can cause interference to neighbouring femtocell and to its users, bilaterally.

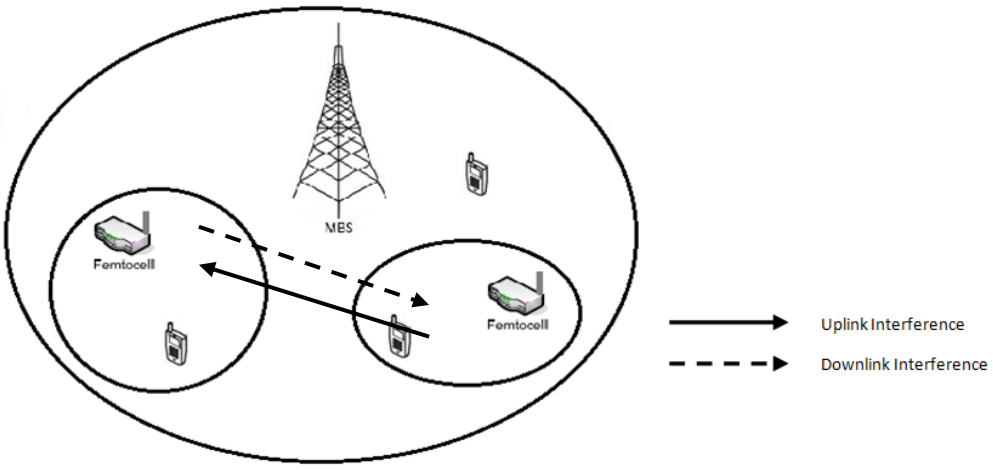

Figure 2.10. A scenario showing co-tier interference between neighbouring femtocells

The uplink co-tier interference is arised from the femtocell user equipments. Femtocell user equipments act as a source of interference. Conversely, the downlink co-tier interference is caused by neigbouring FAP. In this case, user equipments suffer from strong interference. Co-tier interference largely depends on the access mode being used. In closed access mode, users are more susceptible to interference than the other access methods because unsubscribed users cause to dead zones in coverage areas of closed access FAPs [7].

2.2.3.4.2. Cross-tier Interference

This type of interference takes place among network elements that belong to the different layer of the network. User equipments and MBS or FAP can cause interference to the devices located in different layer. Cross-tier interference is illustrated in Figure 2.11.

The uplink cross-tier interference originates from user equipments. Especially, as the macrocell user equipment which is near to the FAP transmits high power signal to communicate with MBS, FAP is affected in a negative manner. On the other hand, the downlink cross-tier interference can take place when MBS and FAP act as a source of interference. In order to cope with interference, spectrum splitting seems to be complete solution. But this is not a cost effective way from the operator's point of view [7].

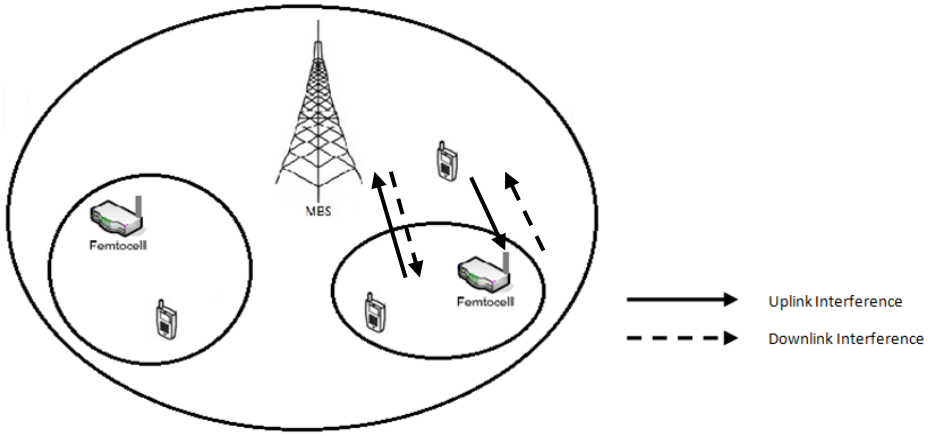

Figure 2.11. A scenario showing cross-tier interference between femtocell and macrocell layers

CHAPTER 3

POWER CONTROL TECHNIQUE

Most of the studies over power control in cellular networks date back to the 90s with a series of results that provide optimum solution for the basic problem formulation, in which transmit power is the only variable, constrained by target SINR values and accordingly optimized to minimize the total power. In this way, power control method has become an eligible position in assisting users who experience poor channels and in limiting interference caused to neighboring cells [34].

Interference management in two-tier networks faces some practical challenges from lack of the coordination between macrocell network and femtocell network due to ad-hoc nature of the femtocell access points (FAPs). In order to increase efficiency of the spectrum usage, it is clear that operators tend to operate the macrocell and femtocells in a common spectrum. But this gives rise to the cross-tier interference between femto and macro layer. Open access mode of femtocell, in which users from different types of network layer can connect, is one such solution for cross-tier problem. A drawback of open access scheme is the need for sufficient backhaul capacity and to protect the home user who pays for this service from being suffered by undesirable costs. In closed access mode, only subscribed users can access to the femtocell service and the other unsubscribed users experience strong degradation in their services. Except for public areas such as airport, campus and shopping malls, closed access mode of femtocells is likely to be preffered from the aspect of private security consideration when compared to the other mode. However, as mentioned before, cross-tier interference might significantly degrade system performance. In this case, special power control schemes can be implemented. For instance, a FAP, which is near the macrocell user devices, transmits high power signal to meet the target SINR values of its served users. This may lead to excessive cross-tier interference to nearby macrocell user. Therefore, it is inevitable for FAPs to develop an effective power control method to avoid the interference and improve the energy efficiency.

Power control is a key technique for interference avoidance, especially in densely deployed femtocell environments. Actually in that method, the focus is on

reducing transmission power of femtocell. When transmission power of a femtocell is controlled and optimised, the macrocell user nearby of the femtocell can be protected from interference. Transmit power optimisation is done in such a way that both femtocell users achieve their required SINR and macrocell users do not experience signal degradation. This also enables FAPs not to waste energy. Additionally, since MBS and FAP make use of entire bandwidth, power control has an advantage over a great majority of interference avoidance techniques [7].

Power control method is divided into two modes. In open loop mode, femtocell adjusts its transmission power based on its measurements results or predetermined system parameters. In closed loop mode, femtocell adjusts its transmission power based on the coordination with macrocell [2]. As for dense deployment environment, another related concept for power control is named as cluster basis in which initial power settings for femtocells is done opportunistically depending on the number of active femtocell in a cluster [35]. For this purpose, centralized sensing is used and represents the fact that MBS can estimate the number of active femtocells per cluster and give information to them for initial power settings. Alternatively, distributed sensing means that each cell senses if the others are active in the same cluster and, then, adjusts its initial power correspondingly [2].

3.1. Power Control for Single Femtocell

In this work, a simple power control technique with single femtocell is evaluated. It is assumed that transmission power of the femtocell is variable and it is aimed at the fact that user equipments in an environment are achieved their target SINR values by adjusting transmission power of the femtocell depending on distances of the UEs to the FAP. In this way, downlink interference problem resulting from FAP is addressed and solved by considering data rate requirements at both the MUE and FUE.

3.1.1. System Model

In order to analyse the system accurately, a simple wireless network model is used as a basis for this work. This model is formed of two layer of network, one is macrocell and the other is femtocell network layer as illustrated in Figure 3.1.

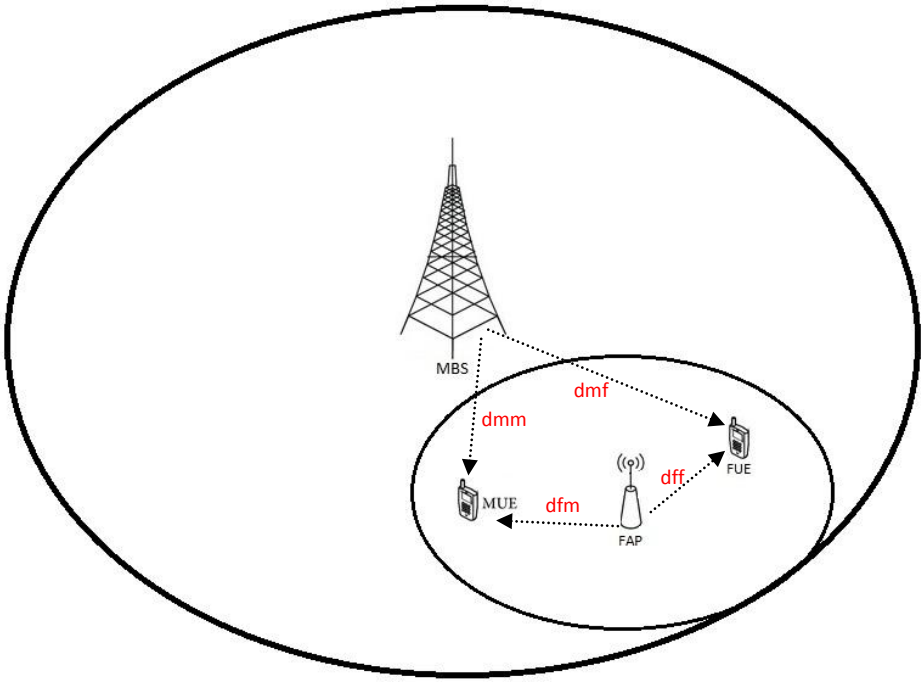

Figure 3.1. Wireless network model for single femtocell

As seen, in the system, there are one macro base station (MBS) with transmission power P^{tm} and one femtocell access point (FAP) with transmission power P^{tf} and its user equipments correspondingly. The distances are denoted by dmm, dmf, dff and dfm which correspond to the distances between MBS and macro user equipment (MUE), MBS and femtocell user equipment (FUE), FAP and FUE, FAP and MUE, respectively.

3.1.1.1. Power Control Optimization Problem for Single FAP

Given that the SINR of MUE is γ^m and the SINR of FUE is γ^f , downlink power control problem for power efficiency maximization and interference avoidance is formulated as follows [36].

$$\min (P^{tf}) \tag{3.1}$$

subject to

$$\gamma^{m} \geq \gamma^{mtar} \tag{3.2}$$

$$\gamma^{f} \geq \gamma^{ftar} \tag{3.3}$$

$$P^{f\min} \leq P^{tf} \leq P^{f\max} \tag{3.4}$$

where γ^{mtar} and γ^{ftar} are the target SINR for the MUE and FUE, respectively. $P^{f\min}$ and $P^{f\max}$ are the minimum and maximum allowable transmission power of the FAP. By means of this formulation, constraints that have been written above enable not only macrocell users to be prevented from downlink interference but also femtocell to maximize its power efficiency. The solution of this problem also provides the required data rate for all the users.

To check the feasibility of the downlink interference problem, we have to write down SINR equations and see if the transmission power of FAP satisfies Equation (3.4). It is assumed that P_r is the average received power. Path loss, shadowing and multipath are all denoted by PL^{ff}, from FAP to FUE, PL^{fm}, from FAP to MUE, PL^{mm}, from MBS to MUE, PL^{mf}, from MBS to FUE. SINR formula in general is written as

$$\gamma = \frac{P_r}{P_I + N_0 B} \tag{3.5}$$

In accordance with the abovementioned assumptions, the SINR of MUE is

$$\gamma^{m} = \frac{P^{tm} / PL^{mm}}{P^{tf} / PL^{fm} + \mathrm{N}_0 B} \tag{3.6}$$

and the SINR of FUE is

$$\gamma^{f} = \frac{P^{tf} / PL^{ff}}{P^{tm} / PL^{mf} + N_0 B} \tag{3.7}$$

These SINR equations, when substituted into (3.2) and (3.3), give knowledge of feasible transmission power range. In other words, in order to satisfy the two constraints on the SINR values in inequalities (3.2) and (3.3), maximum and minimum tranmission

power of FAP can be found by substituting Equations (3.6) and (3.7) into (3.2) and (3.3), as follows.

$$P^{tf} \leq \left[\frac{P^{tm}}{PL^{mm} \quad \gamma^{mtar}} - N_0 B \right] PL^{fm} \tag{3.8}$$

and

$$P^{tf} \geq \left[\frac{P^{tm}}{PL^{mf}} + N_0 B \right] \gamma^{ftar} \; PL^{ff} \tag{3.9}$$

If Equations (3.4), (3.8) and (3.9) is satisfied, the downlink power control problem is feasible.

By using the transmission power of the macrocell base station (P^{tm}) , the target SINR values of FUE and MUE (γ^{ftar} and γ^{mtar}) and the distances (dmm, dmf, dff, dfm), feasibility condition is formulated as

$$\max\{P^{f\min}, \underline{P^{tf}}\} \leq P^{tf} \leq \min\{P^{f\max}, \overline{P^{tf}}\} \tag{3.10}$$

where $\underline{P^{tf}} = \left[\frac{P^{tm}}{PL^{mf}} + N_0 B \right] \gamma^{ftar} \; PL^{ff}$ and $\overline{P^{tf}} = \left[\frac{P^{tm}}{PL^{mm} \quad \gamma^{mtar}} - N_0 B \right] PL^{fm}$.

It follows from the condition above that it is designed to make the most of transmission power efficiency of the femtocell by reaching an optimum transmit power value. $\overline{P^{tf}}$ and $\underline{P^{tf}}$ are our maximum and minimum optimal transmission powers. Feasible transmission power range is constricted by these calculated parameters. These parameters also make it possible for FAP to get more and more efficiency from its emitted-energy. Considering the situation that in feasibility condition (3.10) the maximum allowable transmit power of femtocell ($P^{f\max}$) is greater than the maximum optimal transmit power ($\overline{P^{tf}}$), in that case, femtocell selects lower one ($\overline{P^{tf}}$). On the other hand, considering the situation that the minumum allowable transmit power of femtocell ($P^{f\min}$) is lower than the minimum optimal transmit power ($\underline{P^{tf}}$), in this case, femtocell decides on greater one ($\underline{P^{tf}}$).

In two cases above-mentioned, it goes to show that the feasible power condition in (3.10) provides FAP with not only efficient power selection, making FAP select lower one ($\overline{P^{tf}}$), but also power level which satisfies its users with higher data rates by selecting greater one ($\underline{P^{tf}}$).

3.1.2. Simulation Results

In this section, parameters that have been used in the course of evaluation of single femtocell power control process are shown and the performance of this proposed technique is examined. Simulation parameters are given in Table 3.1.

Explanation	Parameters	Value
Transmission power of MBS	P^{tm}	43 dBm
Transmission power of FAP	P^{tf}	Variable
Maximum allowable transmission power	$P^{f\max}$	23 dBm
Minimum allowable transmission power	$P^{f\min}$	0 dBm
Target SINR values of MUE	γ^{mtar}	0 , 10 dB
Target SINR values of FUE	γ^{ftar}	0 , 10 dB
Number of antenna for MBS	N^{tm}	1
Number of antenna for FAP	N^{tf}	1
Noise power spectral density	N_0	-174 dBm/Hz
Bandwidth	B	10 MHz
Shadowing variance for MBS	σ_m^2	4
Shadowing variance for FAP	σ_f^2	2

Table 3.1. Simulation parameters

In order to understand how the transmission power of femtocell range changes with location of MUE and FUE by providing the feasibility condition given in Equation

(3.10), a simulation results are shown in Figure 3.2 and Figure 3.3. Both figures are intended for the same purpose. However, Figure 3.2 is presented when the target SINR values are 0 dB while Figure 3.3 is presented when the target SINR values are 10 dB. In these figures, solid line represents the maximum optimal transmit power ($\overline{P^{tf}}$) while dashed lines represent the minimum optimal transmit power ($\underline{P^{tf}}$). The distances, dff and dfm, is used to show the changes due to the fact that dff and dfm is the function of $\underline{P^{tf}}$ and $\overline{P^{tf}}$, respectively. For this reason, any change of dff determines only $\underline{P^{tf}}$ in this figure. It is observed that there exist a reasonable range of feasible transmission power for FAP when MUE is at least 5 meters away from FAP and FUE is close to FAP enough. Feasible power interval is between dashed line and solid line at a given distances provided that solid line is upwards of dashed one. Otherwise, this area is regarded as deadzone for MUE. As seen in figure, the feasible range of P^{tf} grows as dff reduces or dfm increases accordingly.

It can be also inferred from this figure that when MUE is closer than FUE to the femtocell, macrocell deadzone comes into being straightforwardly and power control problem does not work well. This is an important drawback of power control technique and needs to be done in such cases. In this thesis, this problem has been addressed and dealth with in the succeeding sections.

Figure 3.4 shows the SINR summation of FUE and MUE variation with respect to the distances, dff and dfm. It is observed that dff and dfm have the dominant effect on the sum of the SINR values. As seen, the total SINR is directly proportional to the distance between FAP and MUE (dfm) while inversely proportional to the distance between FAP and FUE (dff). It can also be inferred from the figure that at the distances where the MUE is approximately 20-30 meters away from the FAP, the total SINR begins to show a significant degradation and this continues as dfm decreases.

Deadzones threatening macrocell users which are located in near field of femtocells make it harder for power control technique to work properly. In the case that MUE is closer than FUE to the nearby FAP, this phenomenon, called Macrocell Deadzone, occurs and has negative impact on the macrocell users. In Figure 3.5 seen as

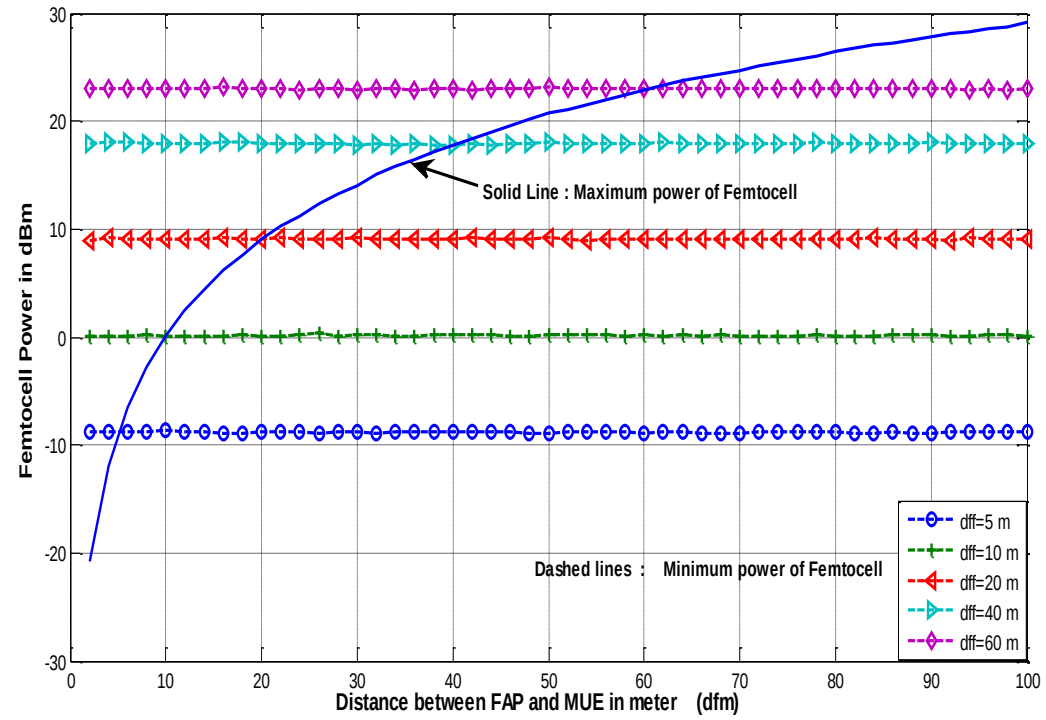

Figure 3.2. The feasible transmission power of FAP for 0 dB-target SINR values

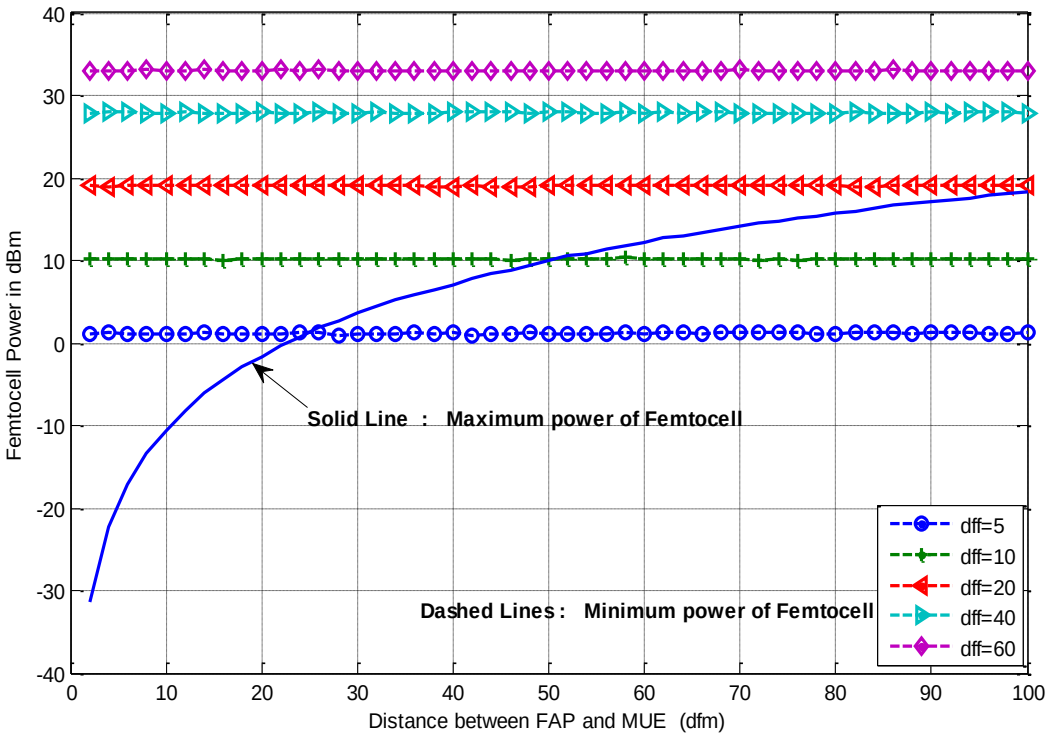

Figure 3.3. The feasible transmission power of FAP for 10 dB-target SINR values

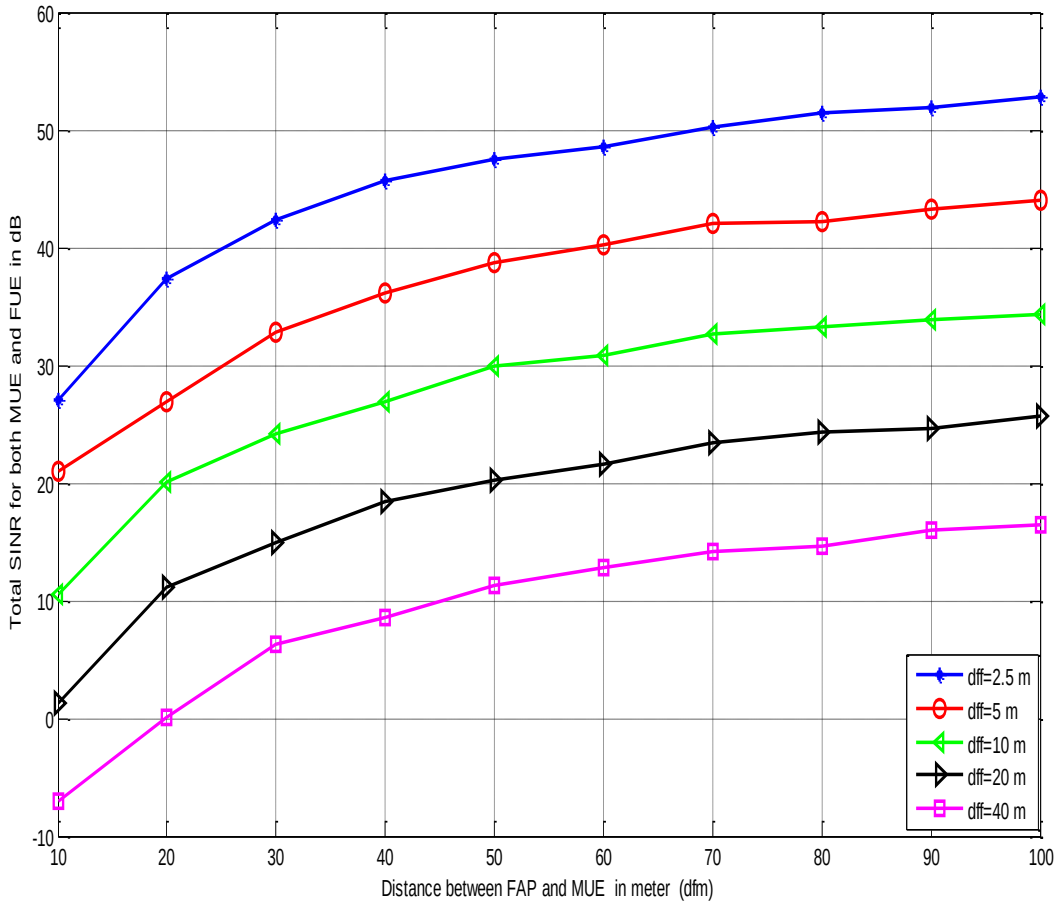

Figure 3.4. Total SINR values vs. Distances, dfm and dff

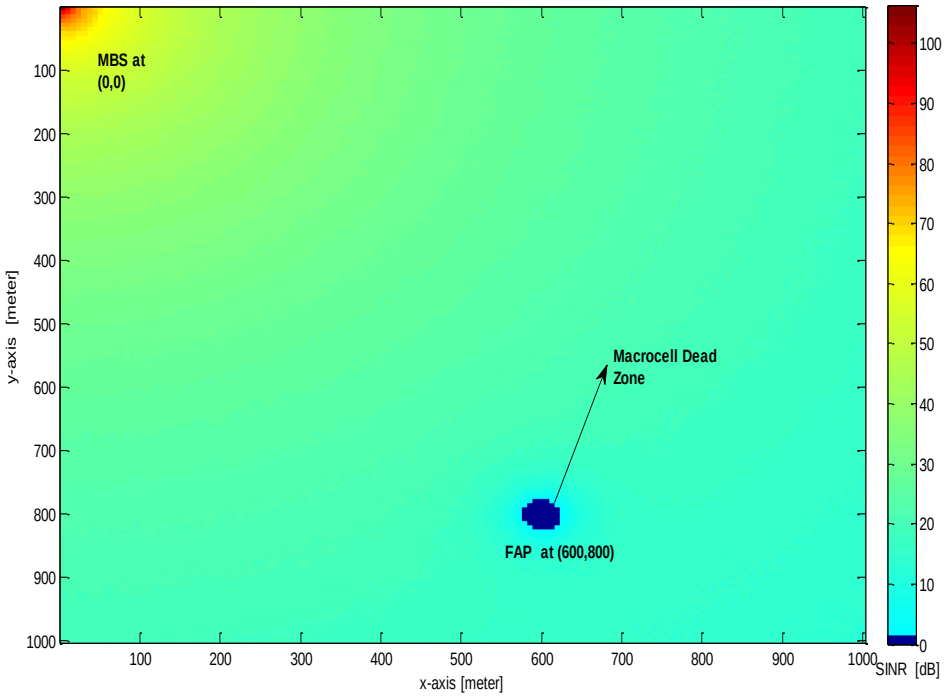

Figure 3.5. SINR map of MUE and Deadzone for MUE when dff = 20 m

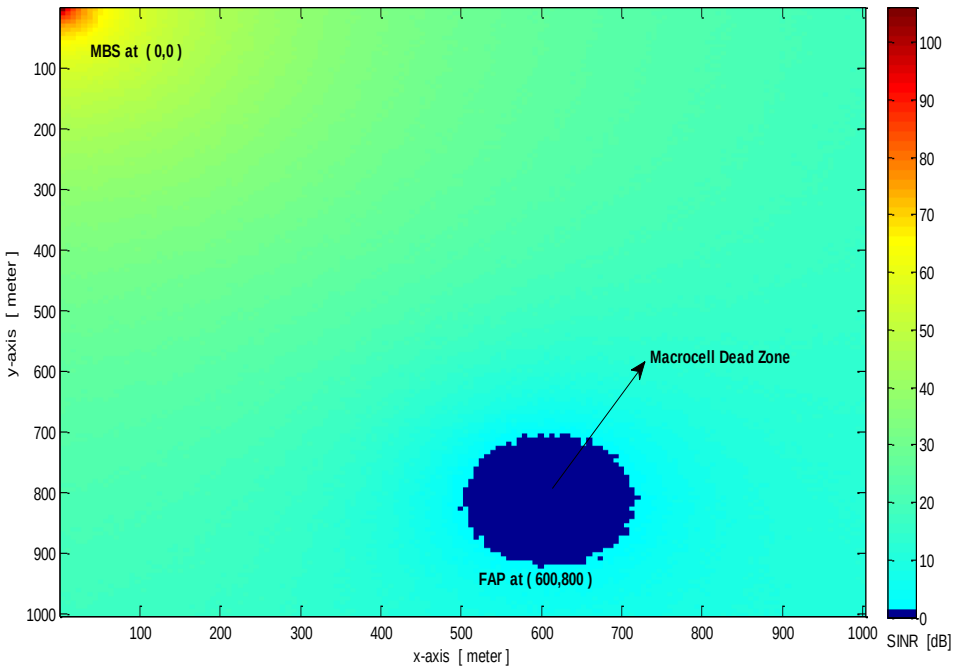

Figure 3.6. SINR map of MUE and Deadzone for MUE when dff = 100 m

a colormap, it is illustrated the degree to which the location of femtocell user affects the size of Macrocell deadzone in power control algorithm. To realize this deadzone, colors in figure represents the SINR value of MUE. Colorbar, on right side of the figure, shows corresponding SINR levels. In here, dark blue indicates the region of SINR values which are under the target SINR value of MUE. When FUE is 20 meters away from FAP, created-deadzone for MUE is clearly seen in the near field of femtocell.

To broaden the scope of this figure, the following figure, Figure 3.6, illustrates the same parameter with different distance from FUE to FAP (dff). It goes to show that when dff is increased to 100 meters, how dramatically Macrocell Deadzone develops and effects MUEs in the region at issue. As seen in two figure, the radius of deadzone is almost the same as the distance of FUE to FAP. It is because power control algorithm adjusts minimum FAP power with respect to its closest user (FUE) that the macrocell deadzone is created accordingly. Also, the maximum power of femtocell is adjusted with respect to the closest MUE as seen in Figure 3.2 and Equation (3.8).

That being said, in order for the power control technique to work properly, MUE must locate in FAP region on the condition that it is not much closer to the FAP than FUE. Otherwise, power allocation does not work and required SINR values is not being satisfied for users. That is regarded as a major drawback of this technique. However, in other cases, power control approach works sharply and provides power-efficient solution for femtocells in terms of Equation (3.10).

3.2. Power Control for Multiple Femtocells

Power control method in multiple femtocells environment is carried out in this section. The scenario is the one that four femtocells are placed in the single macrocell environment and each femtocell and macrocell have one user. Different downlink interference schemes, from femtocells to the macro user, are examined by using different layouts for macro user in the area. Thus, in order to satisfy target SINR values of every user in the system, how the tranmission powers of the femtocells change is determined in compliance with the MUE’s location.

3.2.1. System Model

The network layout scheme to be used in this multiple femtocell work is shown in the Figure 3.7, below.

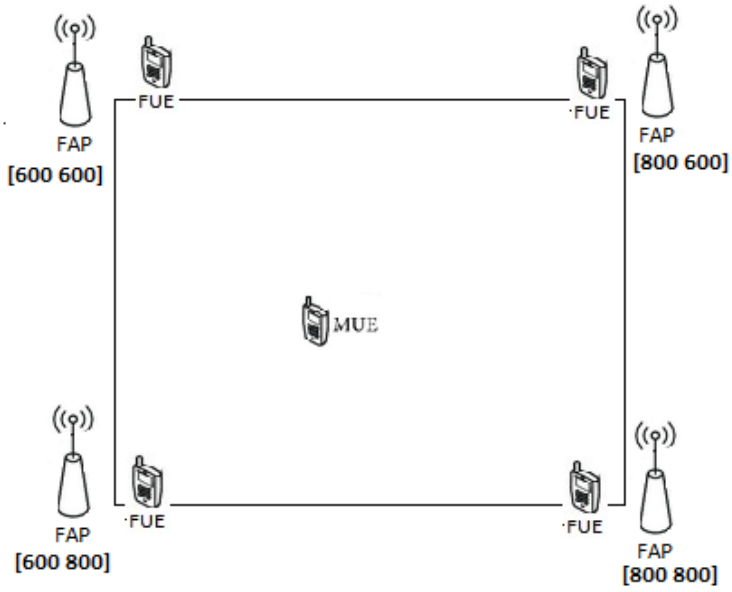

Figure 3.7. Wireless network model for multiple femtocells

Femtocells are located in coordinate axis as their coordinates are shown in abovementioned figure in a way that they constitute a square. It assumed that macrocell base station is in the origin [0 0]. User equipments have variable location on the condition that FUEs are closely placed to their FAPs.

3.2.1.1. Power Control Optimization Problem for multiple FAPs

Based on these network model, problem formulation makes sure that interference on MUE is dealt with in accordance with the required SINR values of users. For this purpose, power control problem can be formulated in general as

$$\min (P_k^f) \qquad ; \qquad k = 1,...,4 \tag{3.11}$$

subject to

$$\gamma^{m} \geq \gamma^{mtar} \tag{3.12}$$

$$\gamma_k^{f} \geq \gamma_k^{ftar} \quad ; \quad \forall k \tag{3.13}$$

$$P^{f\min} \leq P_k^{f} \leq P^{f\max} \quad ; \quad \forall k \tag{3.14}$$

where γ^{mtar} and γ^{ftar} are the target SINR for the MUE and FUE, respectively. $P^{f\min}$ and $P^{f\max}$ are the minimum and maximum allowable transmission power of the FAP. "k" represents individual femtocell number of four femtocells and their users. This formulation is general and the same as the previous single power control technique because the aim is same in general. However, in multiple femtocell scheme, first, the maximum received interference power on MUE from femtocells is calculated. Then, this calculated-power is shared among femtocells by means of a coefficient which is respectively determined with respect to their distances to the MUE.

In the multiple femtocell environment, the SINR formulation of MUE and FUEs are shown below.

$$\gamma^{m} = \frac{P^{tm} / PL^{mm}}{\sum_k (P_k^{f} / PL_k^{fm}) + \mathrm{N}_0 B} \tag{3.15}$$

$$\gamma_k^{f} = \frac{P_k^{f} / PL_{k,k}^{ff}}{\sum_{j \neq k} (P_j^{f} / PL_{j,k}^{ff}) + P^{tm} / PL_k^{mf} + \mathrm{N}_0 B} \tag{3.16}$$

where PL^{mm} is the path loss from macrocell to the MUE, PL_k^{fm} is the path loss from k^{th} femtocell to the MUE. In addition to that, $PL_{k,k}^{ff}$ indicates path loss from femtocell to its own user while $PL_{k,j}^{ff}$ indicates path loss from femtocell to the other FUEs.

Using Equations (3.15) and (3.16) in (3.12) and (3.13) respectively, maximum and minimum transmission power bound is obtained. Thus, the maximum interference power on MUE and the minimum FAP power for the FUEs can be determined by abovementioned process. Firsly, from Equation (3.15), the maximum interference power on MUE is denoted as

$$P_I^m = \sum_k (P_k^f \,/\, PL_k^{fm}) \tag{3.17}$$

This is an aggregate received interference power of MUE. It can also be regarded as a maximum acceptable FAP power for MUE at issue. Using this concept, maximum transmission power bound is written, as follows.

$$P_I^m \leq \left[\frac{P^{tm}}{PL^{mm} \quad \gamma^{mtar}} - \mathrm{N}_0 B \right] \tag{3.18}$$

This equation is obtained from Equation (3.12). It provides the maximum received power from femtocells in total for MUE. At the same time, using the SINR equation of FUE in Equation (3.13), the minimum transmission power bound for each femtocell in the system can be formulated as follows.

$$P_k^{f\min} \quad \geq \quad \left[\frac{P^{tm}}{PL_k^{mf}} \; + \; \mathrm{N}_0 B \right] \gamma^{ftar} \quad PL_{k,k}^{ff} \tag{3.19}$$

Since the cross-tier interference is the only matter involved in, the co-tier interference term, $\sum_{j \neq k} (P_j^f \,/\, PL_{j,k}^{ff})$ in SINR equation of FUE, is not included in Equation (3.19).

In order to determine in which way each individual FAP adjusts its power so that FAPs do not pose an interference to the MUE, it is necessary to go back to the Equation (3.18). In here, the maximum received interference power for MUE, P_I^m, has been described. Based on this, the total power can be shared among FAPs in a distance-based manner. In order to do this, the coefficient is produced by dividing total interference power to the sum of distances from all the FAPs to the MUE, as follows.

$$coef \quad = \quad P_I^m \Big/ \sum_{k=1}^{4} dfm_k \tag{3.20}$$

This coefficient is used in adjusting the power of femtocells with the help of the formula shown below.

$$P_k^I = coef * dfm_k \tag{3.21}$$

$$P_k^{f\max} = P_k^I * PL_k^{fm} \tag{3.22}$$

Thus, tranmission power sharing for all the FAPs in the area can be done and powers become proportional to the distance to the MUE (dfm).

The result obtained from Equation (3.22) provides a maximum power bound, which is denoted by $P_k^{f\max}$, for femtocells so that they do not cause interference on MUE. At the same time, Equation (3.19) enables all the FUEs to be satisfied with SINR values they had. These two parameters form a feasible power region as seen below.

$$\max\{P^{f\min}, P_k^{f\min}\} \le P_k^f \le \min\{P^{f\max}, P_k^{f\max}\} \tag{3.23}$$

where $P_k^{f\min}$ and $P_k^{f\max}$ are calculated parameter to satisfy the SINR values of all user equipment in the system. $P^{f\min}$ and $P^{f\max}$ are the given parameters written as a constraint in Equation (3.14). This formula, which is written in Equation (3.23) above, represents feasibility condition of multiple femtocell case like single femtocell case before. In case of determining the minimum transmission power for femtocell, of the two powers, $P^{f\min}$ $P_k^{f\min}$, the greater one is chosen. However, of the two powers, $P^{f\max}$ $P_k^{f\max}$, the lower one is chosen when maximum transmission power for femtocell is determined.

It is clear that the feasibility condition mentioned above makes it possible not only for all the user equipments to experience good data rate requirements but also for all the FAPS to make the most of the power-efficiency.

3.2.2. Simulation Results

Parameters that have been used in the proposed power control method for multiple femtocells are the same as the previous single femtocell power control method. In this section, performance of the power control method for multiple femtocell is examined.

Given the order of network model in coordinate axes, the placement of femtocells (FAPs) has a square shape and macrocell (MBS) is at the origin point. That

being the case, in order to see to what extent the proposed method responds to the location of MUE and FUE, Figure 3.8 and Figure 3.9 can be examined in detail. Figure 3.8 and Figure 3.9 represent the same issue. However, the only difference between them is that target SINR values are 0 dB in Figure 3.8 and 10 dB in Figure 3.9. In these figures, the calculated maximum and minimum transmission powers of FAPs, $P_k^{f\max}$ $P_k^{f\min}$, are shown with respect to the distances and the feasibility region can be observed accordingly. It follows from the figure that the maximum transmission power of FAP, shown in solid line, depends on dfm, which is the distance from FAP to MUE, while the minimum transmission power of FAP, shown in marked line, depends on dff, which is the distance from FAP to FUE. The parts of plotting where the solid line is below the marked line indicate the dead zones because the maximum transmission power become lower than the minimum power. This phenomenon, as seen in figure, occurs when MUE is close to the FAP or this phenomenon is greatly likely to occur when FUE moves away from FAP so much. In this case, since FUE becomes so distanced, FAP have to transmit more power to satisfy the FUE, as observed from the dashed lines differing in each different dff, and this causes minimum transmission power of FAP to increase. As a result, dead zone is likely to happen much more in such a case.

The following figures are intended for showing the amount of power distribution of the FAPs. In Figure 3.10, MUE is located at the coordinates of (600,640). This position is closer to the FAP – 1 than the others. As far as the proposed power control method is concerned, it is evident, as seen in figure as well, that FAP – 1 adjusts its power in a way that its transmit power is the lowest one among the others. Additionally, the other FAPs adjust their power with respect to the distance to MUE, as well. All in all, the maximum received interference power for MUE, P_I^m, is shared among all the FAPs in an interference-free manner. This idea goes on to show itself in the other figures to come. In Figure 3.11, FAP - 2 has the lowest power this time. In Figures 3.12 and 3.13, the others are illustrated respectively. All these colormap figures shows how the FAPs share the tranmission power with respect to the distance to MUE in order not to cause an interference.

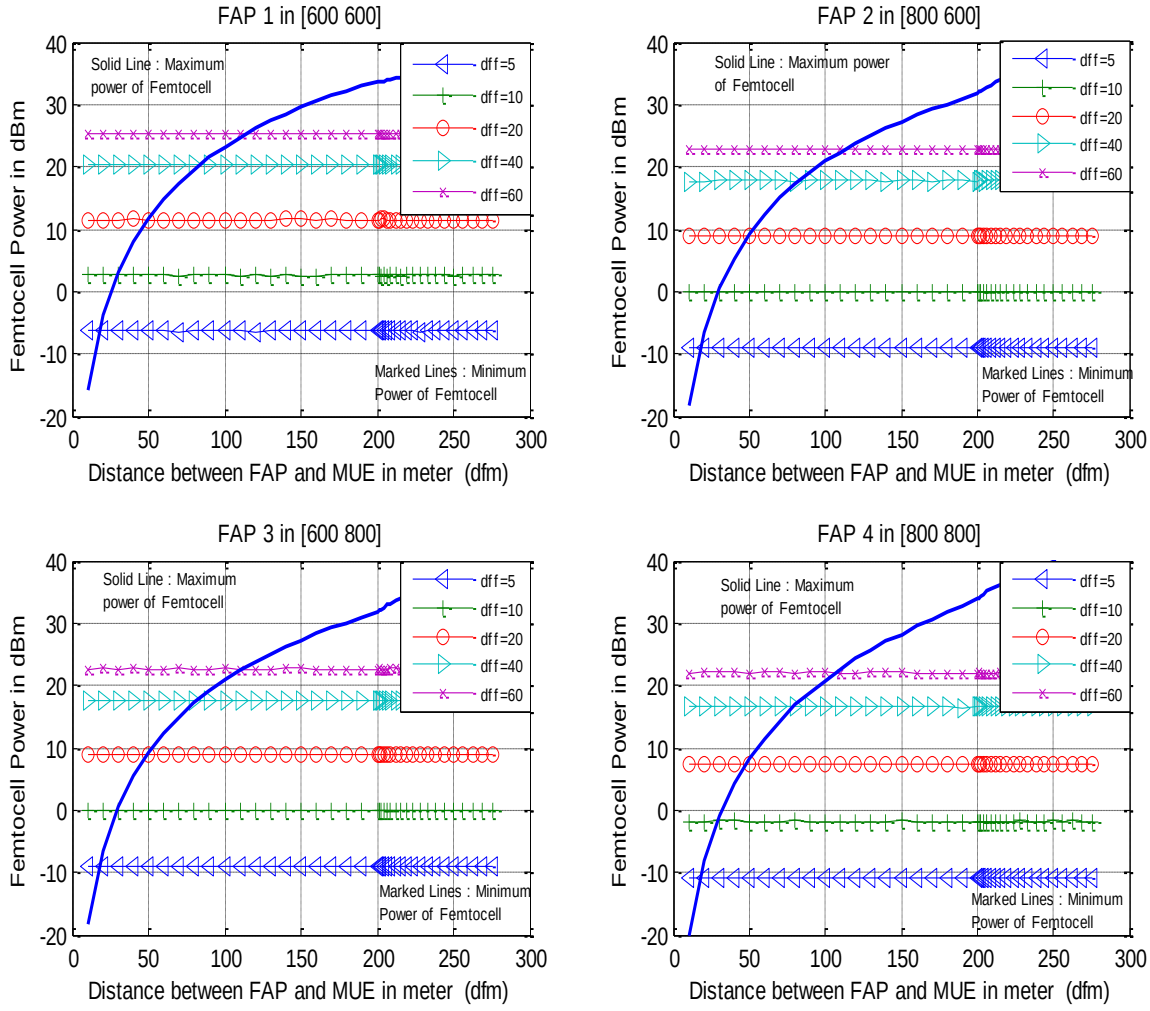

Figure 3.8. The feasible transmission power levels for 0 dB-target SINR value

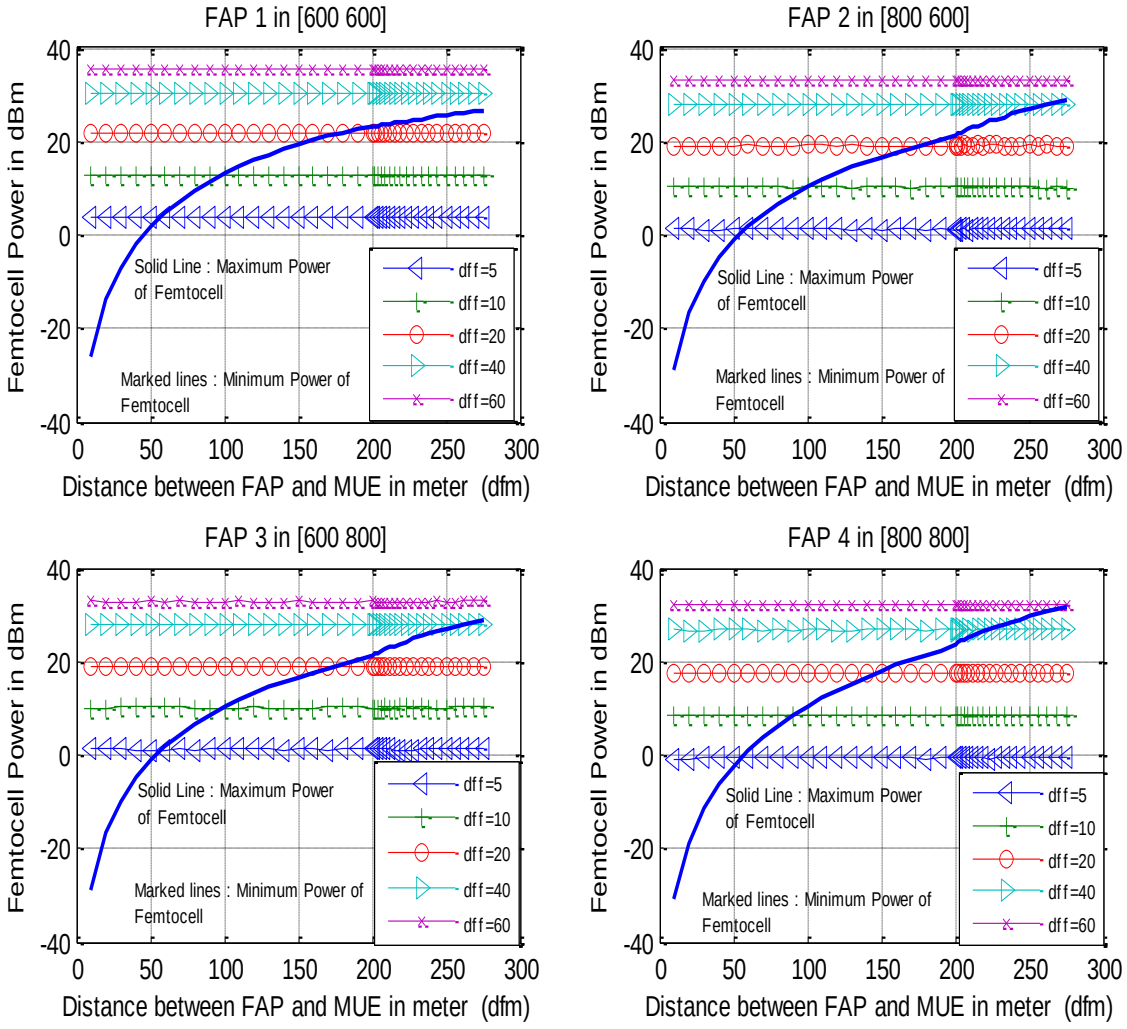

Figure 3.9. The feasible transmission power levels for 10 dB-target SINR value

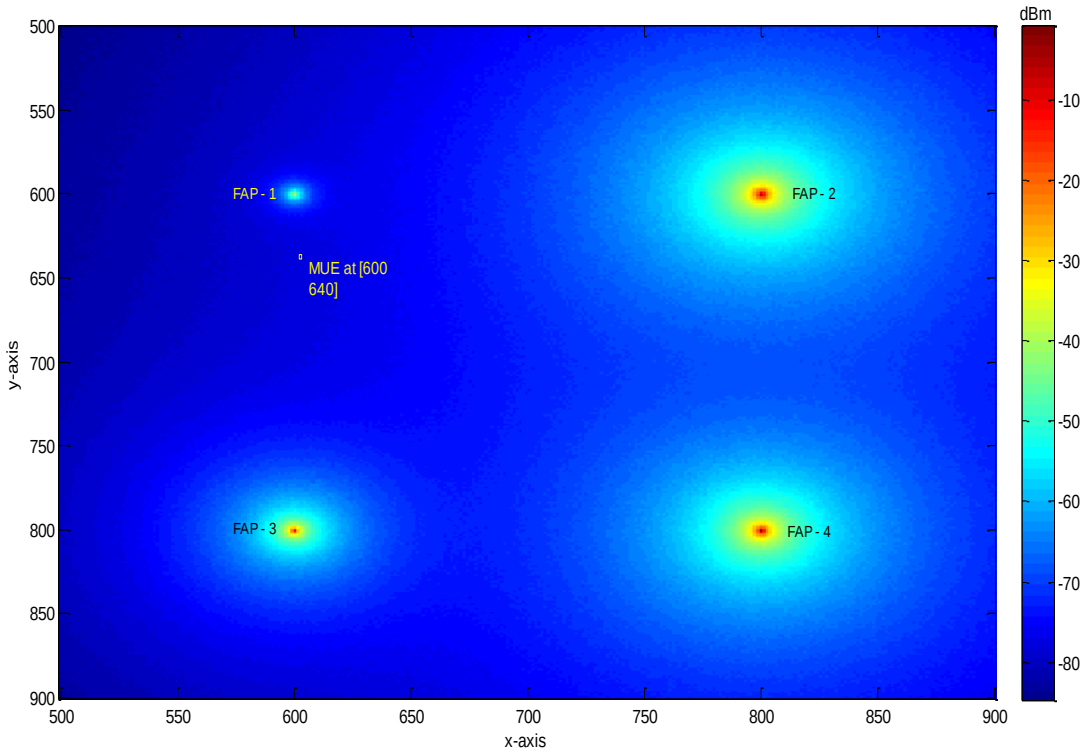

Figure 3.10. The power distribution of the FAPs with MUE at [600 640]

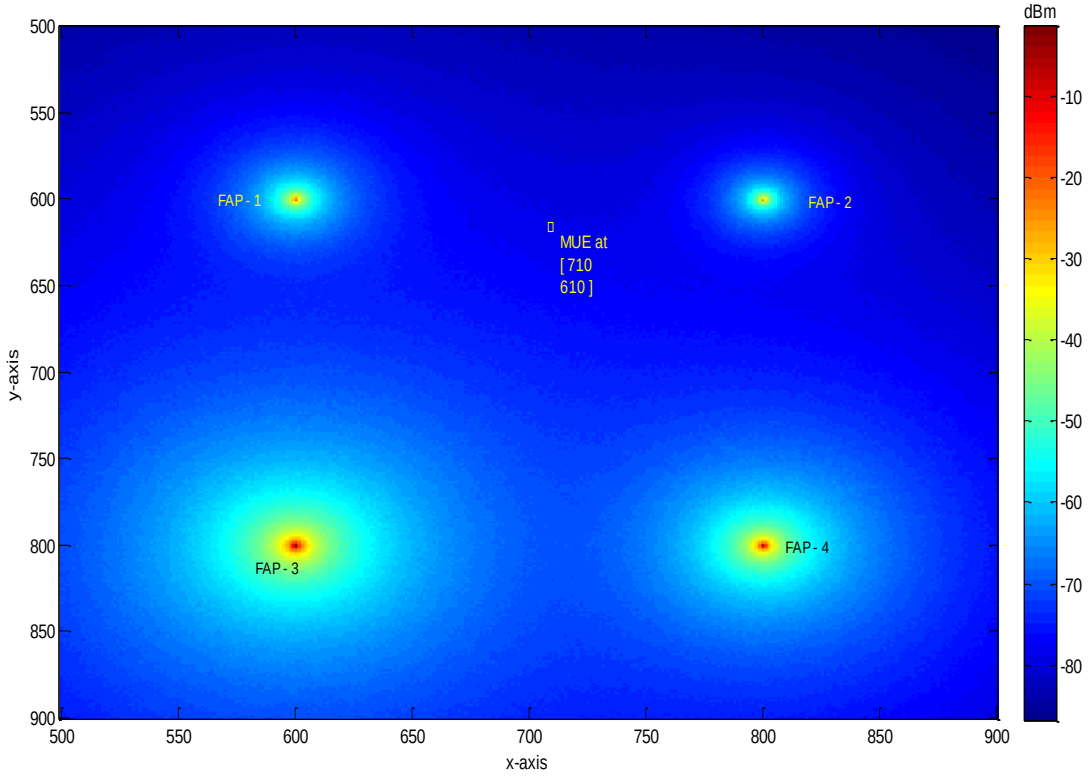

Figure 3.11. The power distribution of the FAPs with MUE at [710 610]

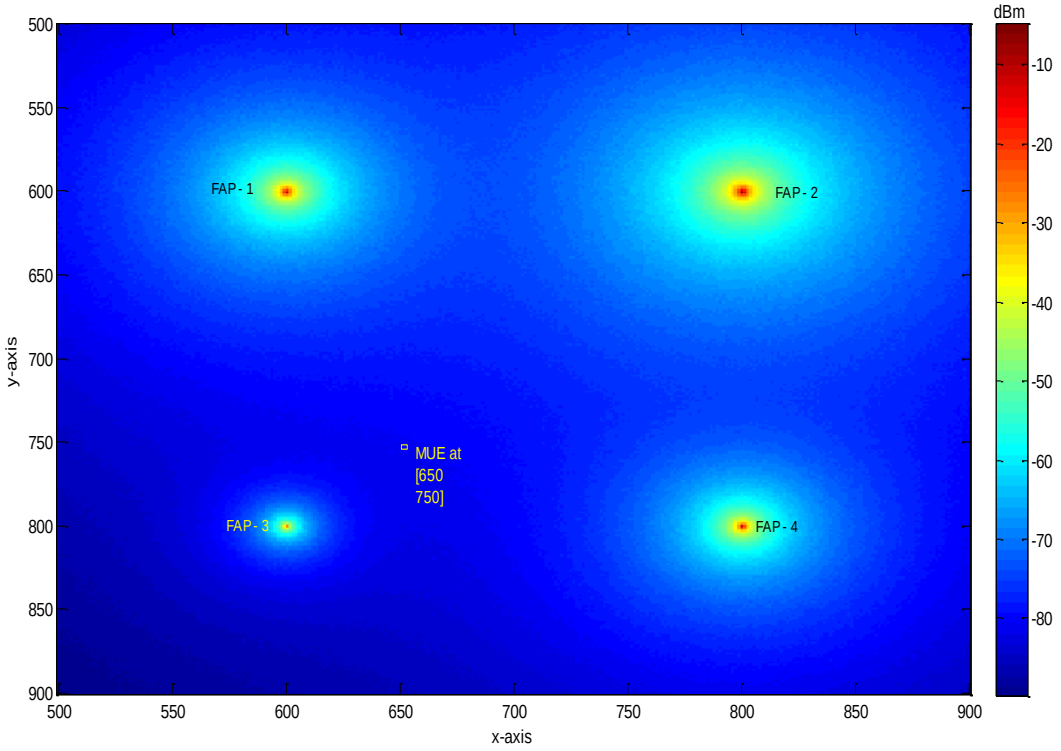

Figure 3.12. The power distribution of the FAPs with MUE at [650 750]

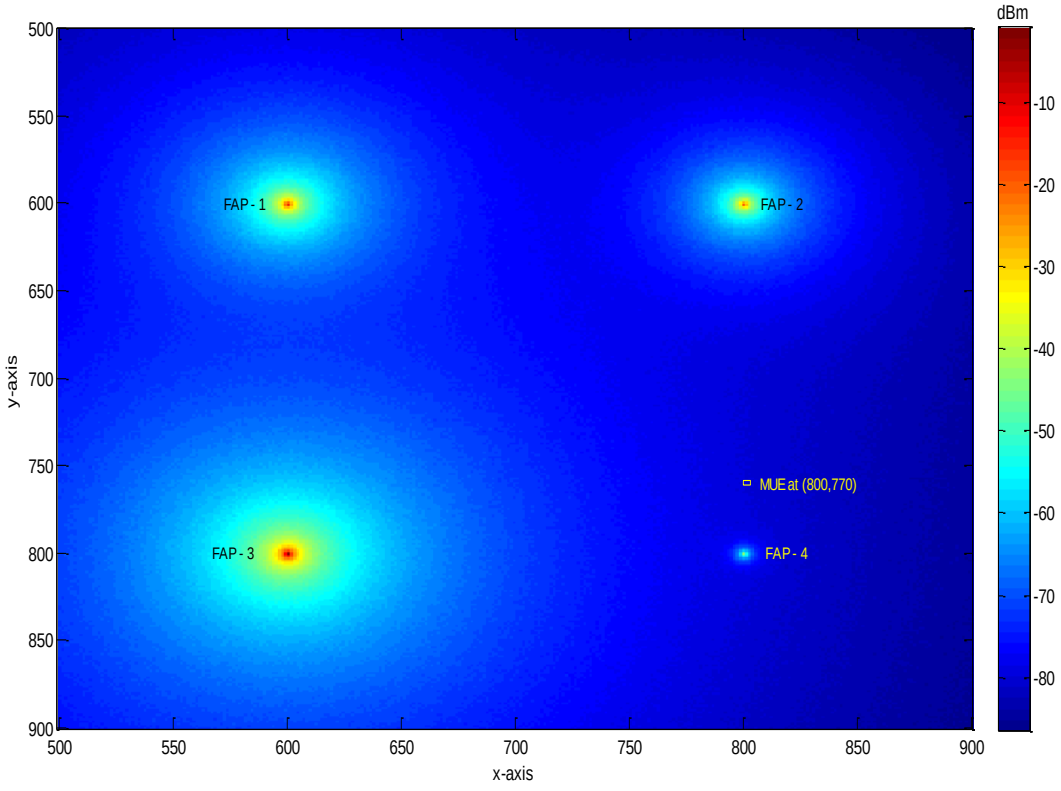

Figure 3.13. The power distribution of the FAPs with MUE at [800 770]

CHAPTER 4

TRANSMIT BEAMFORMING TECHNIQUE

Beamforming is of great importance in terms of interference suppression as well as high data rates and small error rates communication [11]. Due to the fact that beam patterns can be adjusted in a way that desired directions make the most of effective SINR value, this can be used to suppress interference by nulling that interference-causing areas with the help of adjustable-array nature of the beamforming antennas. For this purpose, beamforming weight vectors (**w**) are used [37]. By designing the weight vectors, beam pattern can be guided to desired direction, which makes it easy for transmitting device not to cause any interference to other users. Considering the femtocell case, Figure 4.1 illustrates beamforming process with beamforming weight vectors.

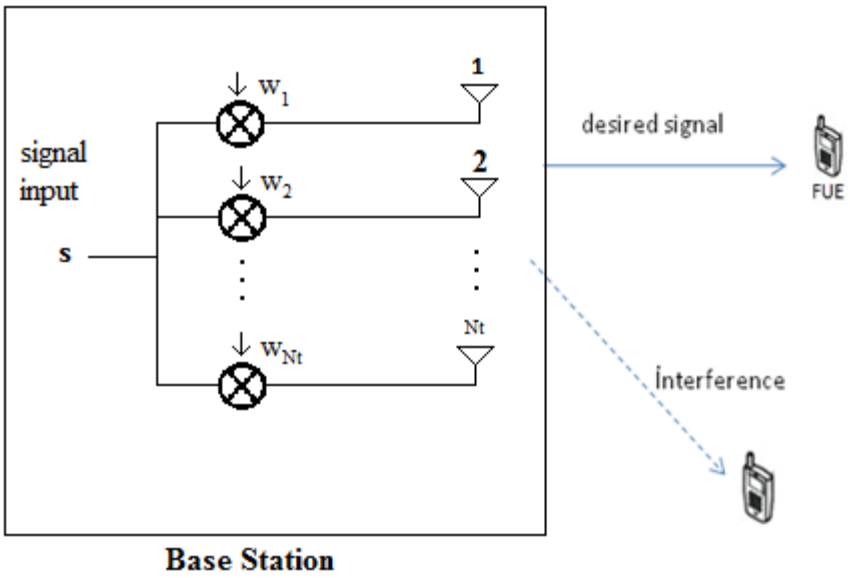

Figure 4.1. Beamforming process

As seen in Figure 4.1, beamforming issue is mostly concerned with the signal processing area. All the process is carried out in transmitter or receiver side. Signal is firstly multiplied by beamforming weight vector and then transmitted by concerned

antenna to the desired direction. How the beamforming weight vector is computed is explained succeeding sections in detail.

Beamforming technique classified into two as transmit and receive beamforming [38]. Both of them are substantially different in nature. Receive beamforming can be applied at each receiver independently. This process does not affect other links in network. However, in transmit beamforming tehnique, any kind of change in beam pattern of transmit antenna can affect all other receivers in that region. As a result, transmit beamforming is implemented jointly in the entire network.

Transmit beamforming technique is performed using two different method. These are zero forcing and maximal ratio beamforming. Maximal ratio beamforming focuses on signal maximization for desired user while zero forcing beamforming focuses on suppression of interference sources. These two method are carried out with the help of beamforming precoding vector, in other words, weight vector. Precoding vector is designed in such a way that either channel vector of desired user can be maximized in the event that interfering base station is too far away or channel vector of interfering user can be suppressed. Suppression process is handled by designing precoding vectors in a way that they are orthogonal to the channel vectors of interfering users.

In this chapter, transmit beamforming with partial zero forcing technique is, first, carried out in single femtocell scenario and then implemented for multiple femtocells environment. Simulation results are also evaluated at the end of the each scenario.

4.1. Beamforming Technique in Single Femtocell

4.1.1. System Model

In this work, transmit beamforming technique is implemented by using partial zero forcing method. It is assumed that the antenna numbers of macro base station and femtocell access point are denoted by N^{tm} and N^{tf}, respectively and base stations are located as shown in Figure 3.1. Moreover, both the macrocell user and femtocell user devices are equipped with single antenna. Thus, a simple multiple-input single-output (MISO) system has been established.

4.1.1.1. Transmit Beamforming Technique with Partial Zero Forcing in Single FAP

Received SINRs for both MUE and FUE, is formulated as follows.

$$\gamma^{m} = \frac{(P^{tm} / PL^{mm} N^{tm}) G^{mm}}{(P^{tf} / PL^{fm} N^{tf}) G^{fm} + \mathrm{N}_0 B} \tag{4.1}$$

$$\gamma^{f} = \frac{(P^{tf} / PL^{ff} N^{tf}) G^{ff}}{(P^{tm} / PL^{mf} N^{tm}) G^{mf} + \mathrm{N}_0 B} \tag{4.2}$$

where (G^{mm}, G^{mf}) *and* (G^{ff}, G^{fm}) are channel gains for macrocell and femtocell user, respectively. This gain is composed of multiplication of channel vector (**h**) and beamforming weight vector (**w**). **h** is a channel vector of $N_t \times 1$ and it is assumed that each component of $\boldsymbol{h}_{u,v}$ has independent identically distributed random variable with CN(0,1). Channel gains are shown in below:

$$G^{mm} = \left| (\boldsymbol{h}^{mm})^{H} \boldsymbol{w}^{m} \right|^2 \tag{4.3}$$

$$G^{mf} = \left| (\boldsymbol{h}^{mf})^{H} \boldsymbol{w}^{m} \right|^2 \tag{4.4}$$

$$G^{ff} = \left| (\boldsymbol{h}^{ff})^{H} \boldsymbol{w}^{f} \right|^2 \tag{4.5}$$

$$G^{fm} = \left| (\boldsymbol{h}^{fm})^{H} \boldsymbol{w}^{f} \right|^2 \tag{4.6}$$

In order to employ zero forcing beamforming to the system, beamforming weight vectors are designed to cancel other user's effect and, in this way, to avoid interference. For instance, $\boldsymbol{w}^{m}$ suppresses the channel vector from MBS to FUE, denoted by $\boldsymbol{h}^{mf}$, whereas maximizing the channel vector from MBS to MUE, denoted by $\boldsymbol{h}^{mm}$. The same design procedure is applied for $\boldsymbol{w}^{f}$. Co-tier channel vectors ($\boldsymbol{h}^{ff}$, $\boldsymbol{h}^{mm}$) is maximized while cross-tier ones ($\boldsymbol{h}^{mf}$, $\boldsymbol{h}^{fm}$) is suppressed. Thus, cross-tier interference is cancelled to a large degree.

Assumed that U is the base station number in an area and N_t is the antenna number, this cancellation process can be done by providing $N_t \geq U$ and satisfying orthogonality criterion, $\boldsymbol{h}_{i,u}^H \boldsymbol{w}_u = 0$ for $\forall i \quad i \neq u$. According to this criterion, beamforming weight vector $\boldsymbol{w}_u$ is selected in the direction of the projection of the channel vector, which is $\boldsymbol{h}_{u,u}$, on the nullspace of $\boldsymbol{V}_u = [\boldsymbol{h}_{u,1}, \boldsymbol{h}_{u,2}, \ldots, \boldsymbol{h}_{u,u-1}, \boldsymbol{h}_{u,u+1}, \boldsymbol{h}_{u,U}]$ with the size of $N_t \times (U-1)$. Then, the precoding vector is determined as follows [39]

$$\boldsymbol{w}_u = (\boldsymbol{I} - \boldsymbol{Z})\boldsymbol{h}_{u,u} \tag{4.7}$$

where $\boldsymbol{Z}$ is the projection matrix on $\boldsymbol{V}_u$ and $\boldsymbol{I}$ is identity matrix. The projection matrix $\boldsymbol{Z}$ is formulated as

$$\boldsymbol{Z} = \boldsymbol{V}_u (\boldsymbol{V}_u^H \boldsymbol{V}_u)^{-1} \boldsymbol{V}_u^H \tag{4.8}$$

Based on abovementioned formulization, in the scope of thesis work, determining of $\boldsymbol{w}^m$ and $\boldsymbol{w}^f$, which are used in Equations (4.1) and (4.2), follows these processes written below. Here, since there are only one macro and one femto base station, U equals to 2. Macrocell beamforming weight vector is found as

$$\boldsymbol{w}^m = (\boldsymbol{I} - \boldsymbol{Z}^m)\boldsymbol{h}^{mm} \tag{4.9}$$

where

$$\boldsymbol{Z}^m = \boldsymbol{V}^m ((\boldsymbol{V}^m)^H \boldsymbol{V}^m)^{-1} (\boldsymbol{V}^m)^H \tag{4.10}$$

and

$$\boldsymbol{V}^m = \boldsymbol{h}^{mf} \tag{4.11}$$

In addition, femtocell beamforming weight vector is found as

$$\boldsymbol{w}^f = (\boldsymbol{I} - \boldsymbol{Z}^f)\boldsymbol{h}^{ff} \tag{4.12}$$

where

$$\boldsymbol{Z}^{f} = \boldsymbol{V}^{f}((\boldsymbol{V}^{f})^{H}\boldsymbol{V}^{f})^{-1}(\boldsymbol{V}^{f})^{H} \tag{4.13}$$

and

$$\boldsymbol{V}^{f} = \boldsymbol{h}^{fm} \tag{4.14}$$

In this way, by producing weight vectors which are orthogonal to the channel vectors, they can be forced to approximately zero by applying Equation (4.4) and (4.6). At the end, SINR values for MUE and FUE in Equations (4.1) and (4.2) is improved with reference to abovementioned operations.

4.1.2. Simulation Results

In thesis work, the system model given in Figure 3.1 is evaluated and simulated by performing only beamforming process. So-called beamforming techniques make it possible for SINR of macrocell user and femtocell user devices to keep on desired values which are important for reliable communication. To do this, cross-tier interference is cancelled by partial zero forcing method. Simulation parameters shown in Table 3.1 is used in this work except that the transmission power of FAP is taken as 23 dB and N^{tm}, N^{tf} equal to 4 and 2, respectively.

To illustrate the degree to which this technique impacts on SINR values, Figure 4.2 and 4.3 are shown in the following pages. Figure 4.2 is intended for SINR variation of MUE with respect to the distance to FAP (dfm). It clearly follows from this figure that applied beamforming technique keeps the MUE's SINR values on desired levels even if MUE is so close to the femtocell. Thanks to the suppression method which cancels the channel vector from nearby femtocell, macrocell user does not depend on distance to the femtocell. In Figure 4.2, the line plotted in red indicates this issue. SINR values of MUE, as seen, has been stabilized on desired SINR values with the help of

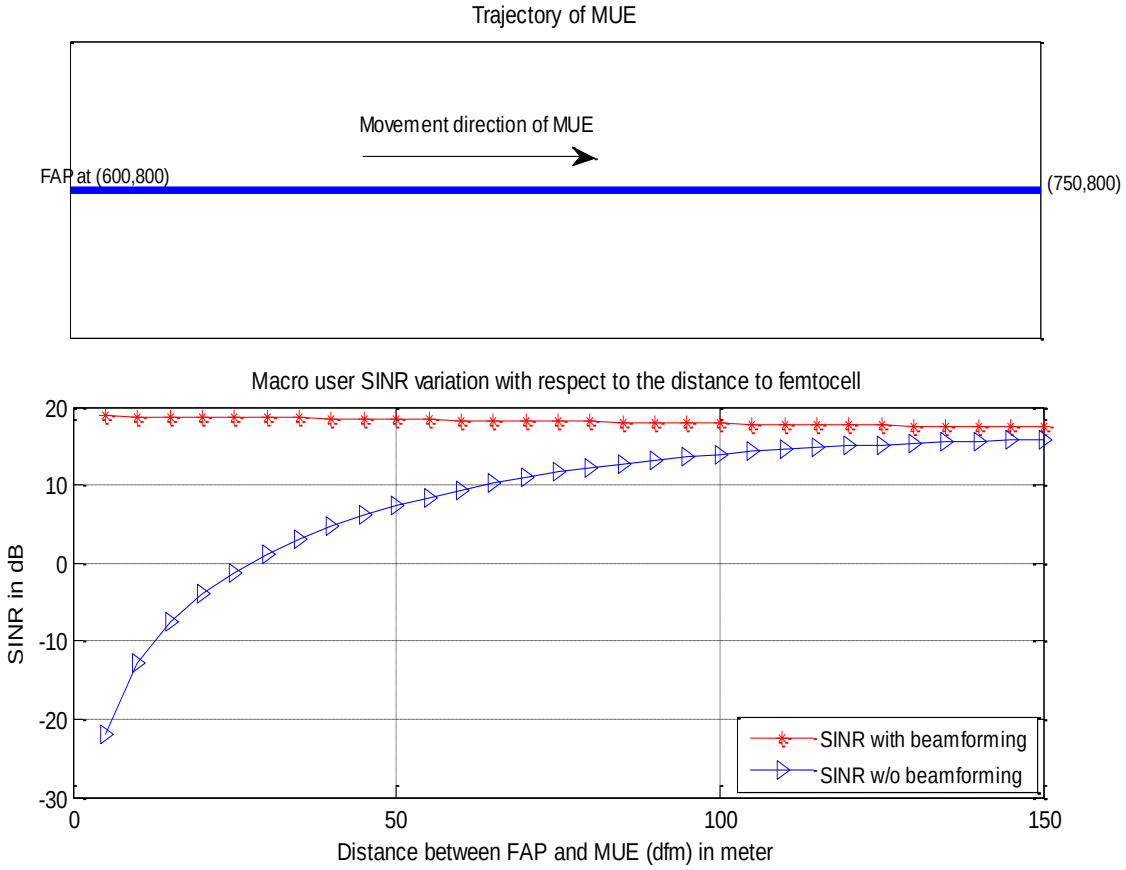

Figure 4.2. SINR of MUE vs dfm with and without beamforming

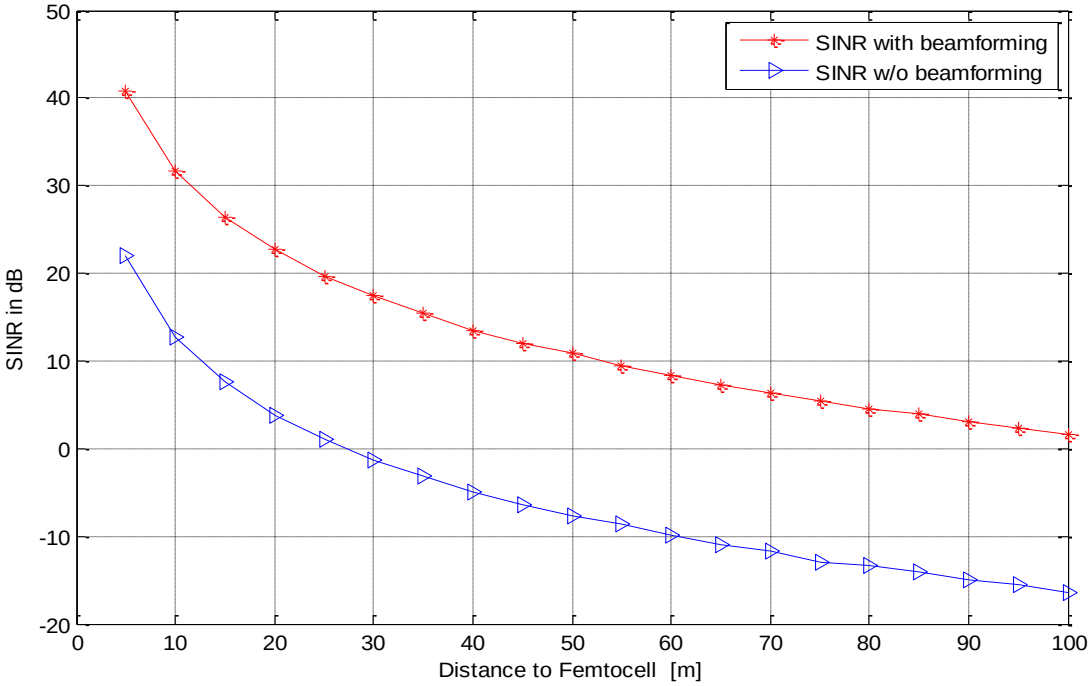

Figure 4.3. SINR of FUE vs dff with and without beamforming

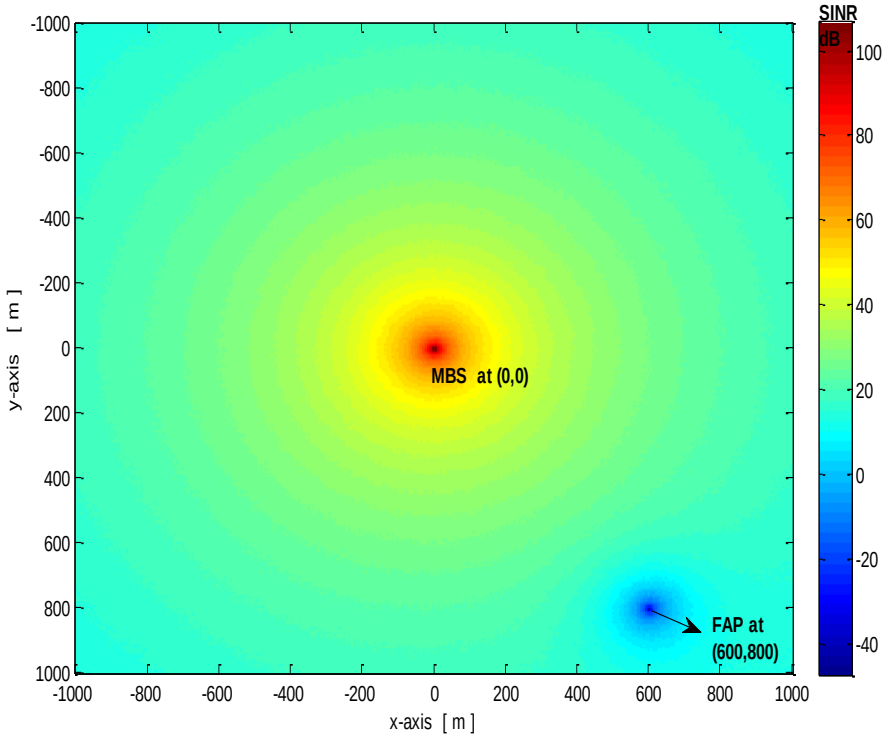

Figure 4.4. SINR distribution of MUE in an area without beamforming

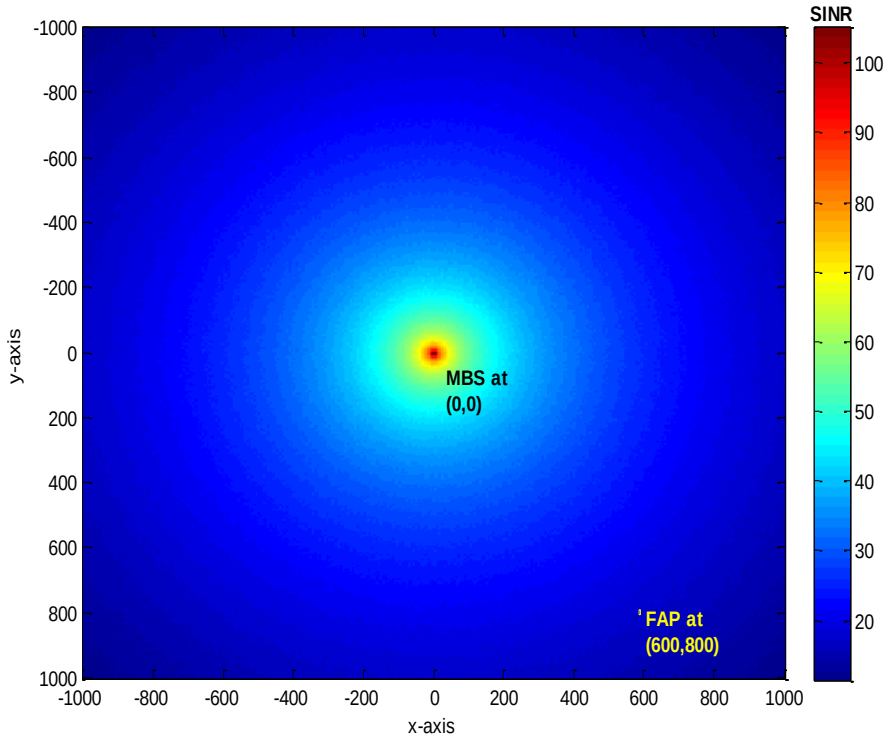

Figure 4.5. SINR distribution of MUE in an area with beamforming

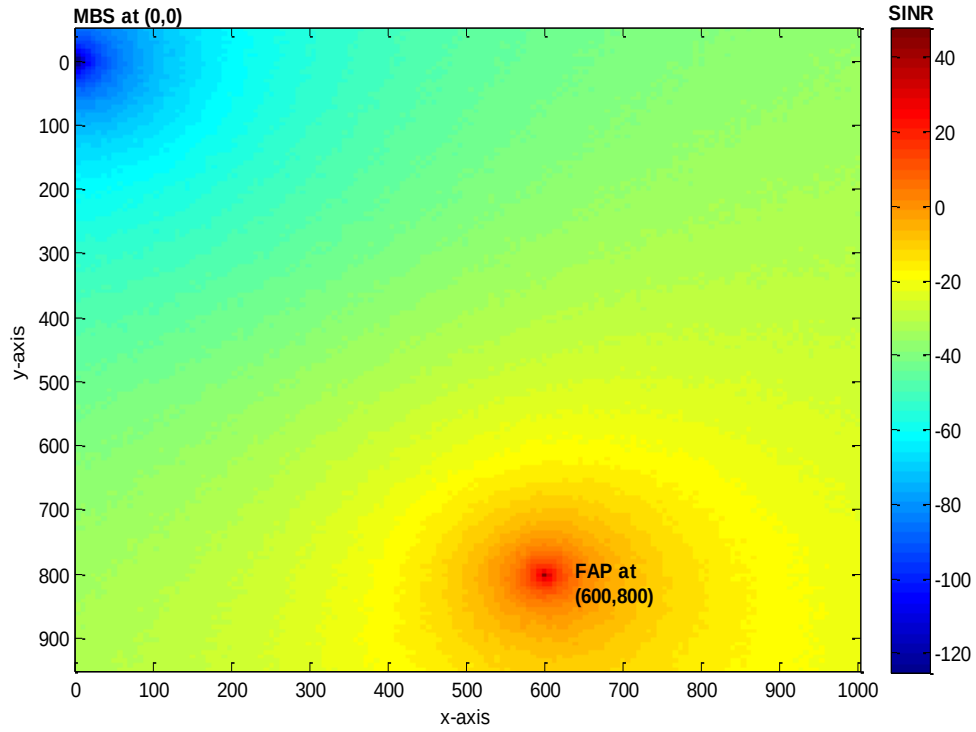

Figure 4.6. SINR distribution of FUE in an area without beamforming

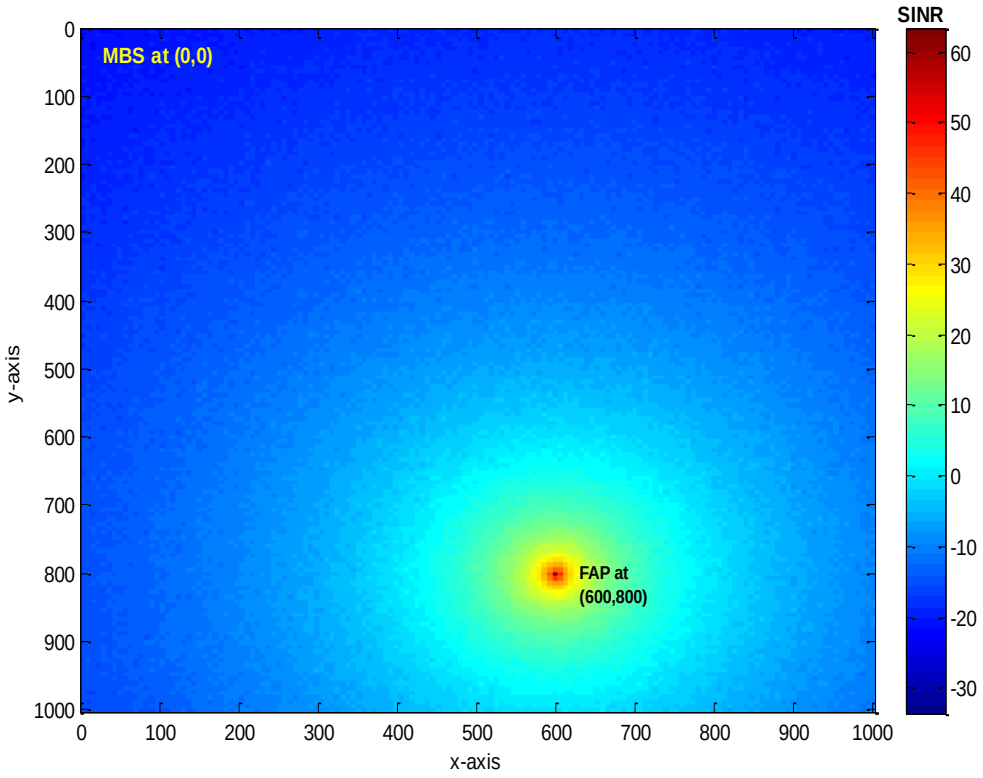

Figure 4.7. SINR distribution of FUE in an area with beamforming

beamforming technique whereas blue line shows decrease as MUE is much closer to the femtocell. As a result, there is no doubt that according to the results, partial zero-forcing beamforming technique completely suppresses cross-tier inteference resulting from femtocell.

In Figure 4.3, it is also shown how the SINR of FUE is improved when beamforming is applied. Considering these two figures, (4.2) and (4.3), it can be inferred that beamforming technique not only suppresses cross-tier interference for MUE but also improves SINR value of FUE.

In Figures 4.4-4.7, overall SINR distributions in macrocell coverage area is illustrated. Two pairs of figures, (4.4-4.5) and (4.6-4.7), are comparable with amongst each other. FAP is located at (600,800) coordinates and its transmission power is assumed to be 23 dBm in these figures. MBS is in the origin point. Figure 4.4 and 4.5 show the MUE's SINR variation in the area and also, Figure 4.6-4.7 show the FUE's SINR distribution with and without beamforming respectively. From the point of view of these figures, it can be seen that without beamforming there is a great degradation effect for both MUE and FUE when they are close to their counterpart interference object, which is MBS for FUE or FAP for MUE. For example, in Figure 4.4, SINR of MUE begins to drop below zero when MUE comes close to FAP approximately 50 meters. But, in other case in which beamforming technique is used, shown in Figure 4.5, any kind of degradation effect of nearby FAP over MUE is not observed. With the help of beamforming technique, interference is completely handled. As it is seen in the images under discussion, SINR values are affected in a positive way. The results of this effect on FUE can be observed when Figure 4.6 and 4.7 is compared.

4.2. Beamforming Technique in Multiple Femtocells

In this section, the scenario in which there are four femtocells or FAPs and one macro base station is formed and beamforming technique is implemented. The main aim here is, like previous ones, to eliminate the cross-tier interference from FAPs to MUE. Implementing the method to that end, it is evaluated how the beamforming method in multiple environment responds. The so-called technique is investigated in two different situation. First, it is applied to one femtocell which has the greatest interference power on MUE. Second, it is applied to two femtocells which have the greatest interference

power on MUE. All the results of two separate situation are shown in simulation results section.

4.2.1. System Model

The system model used in this work is shown in Figure 3.7 in the previous chapter. This scheme consists of four femtocells and one macro base station in the origin point. Each base station has one user. In this scenario, using beamforming technique with partial zero forcing method, cross-tier interference from FAPs to the MUE is only dealt with. Since FAPs are far from each other, there is no interference between FAPs.

4.2.1.1. Transmit Beamforming Technique with Partial Zero Forcing in Multiple FAPs

The main system parameter is SINR values in order to see whether the method works. In the multiple system, the SINR values of users are formulated as follows.

$$\gamma^{m} = \frac{(P^{tm} / PL^{mm} N^{tm}) G^{mm}}{\sum_{k} (P_k^{f} G_k^{fm} / PL_k^{fm} N^{tf}) + N_0 B} \tag{4.15}$$

$$\gamma_k^{f} = \frac{(P_k^{f} / PL_{k,k}^{ff} N^{tf}) G_{k,k}^{ff}}{\sum_{j \neq k} (P_j^{f} G_{j,k}^{ff} / PL_{j,k}^{ff} N^{tf}) + (P^{tm} / PL_k^{mf} N^{tm}) G_k^{mf} + N_0 B} \tag{4.16}$$

where G^{mm} is channel gain between MBS and MUE, G_k^{fm} is channel gain between k^{th} FAP and MUE, $G_{k,k}^{ff}$ is the one between k^{th} FAP and k^{th} FUE, $G_{j,k}^{ff}$ is the one between j^{th} FAP and k^{th} FUE, G_k^{mf} is the one between MBS and k^{th} FUE. Since the co-tier interference is out of scope of thesis, the term in SINR formula of FUE, $\sum_{j \neq k} (P_j^{f} G_{j,k}^{ff} / PL_{j,k}^{ff} N^{tf})$, is not used in further processes and assumed to be zero. The channel gains for macro base station are shown as follows.

$$G^{mm} = \left|(\boldsymbol{h}^{mm})^H \boldsymbol{w}^m\right|^2 \tag{4.17}$$

$$G_k^{mf} = \left|(\boldsymbol{h}_k^{mf})^H \boldsymbol{w}^m\right|^2 \qquad \text{k=1,...,4} \tag{4.18}$$

Here, k denotes the FAP index number. Channel gains for femtocell differ depending on whether FAP is selected for beamforming or not. Formulations are given below.

$$G_{k,k}^{ff} = \left\|\boldsymbol{h}_k^{ff}\right\|^2 \qquad k \neq k^* \tag{4.19}$$

$$G_{k,k}^{ff} = \left|(\boldsymbol{h}_k^{ff})^H \boldsymbol{w}_k^f\right|^2 \qquad k = k^* \tag{4.20}$$

$$G_k^{fm} = \left\|\boldsymbol{h}_k^{fm}\right\|^2 \qquad k \neq k^* \tag{4.21}$$

$$G_k^{fm} = \left|(\boldsymbol{h}_k^{fm})^H \boldsymbol{w}_k^f\right|^2 \qquad k = k^* \tag{4.22}$$

Here, FAP with index k^* is selected for partial zero forcing to cancel interference and beamforming vector is produced accordingly. The other femtocells which are not selected to implement beamforming technique have channel gains as shown in Equations (4.19) and (4.21).

With the help of beamforming vectors, channel gains G_k^{mf} and G_k^{fm} are forced to zero while G^{mm} and $G_{k,k}^{ff}$ are maximized. This is obtained by producing beamforming vectors in a way that they are orthogonal to the cross-tier channel vectors. In this way, beamforming vectors (**w**), as seen above, enable the base stations to adjust their channels gain depending on a user basis, which makes it possible for the FAP not to cause interference to MUE in area.

The abovementioned beamforming vectors for macrocell and femtocell base stations are produced as follows.

$$\boldsymbol{w}_k^f = (\boldsymbol{I} - \boldsymbol{Z}_k^f)\boldsymbol{h}_{k,k}^{ff} \qquad k = k^* \tag{4.23}$$

$$\boldsymbol{w}^m = (\boldsymbol{I} - \boldsymbol{Z}^m)\boldsymbol{h}^{mm} \tag{4.24}$$

where $\boldsymbol{Z}_k^f$ and $\boldsymbol{Z}^m$ are the projection matrices on $\boldsymbol{V}_k^f$ and $\boldsymbol{V}^m$, and formulated as

$$\boldsymbol{Z}_k^f = \boldsymbol{V}_f^k((\boldsymbol{V}_k^f)^H \boldsymbol{V}_k^f)^{-1}(\boldsymbol{V}_k^f)^H \tag{4.25}$$

$$\boldsymbol{Z}^m = \boldsymbol{V}^m((\boldsymbol{V}^m)^H \boldsymbol{V}^m)^{-1}(\boldsymbol{V}^m)^H \tag{4.26}$$

Here, since the beamforming method is implemented for two different cases in multiple FAP study, $\boldsymbol{V}_k^f$ is created in two different ways. When the so-called method is applied to one FAP, $\boldsymbol{V}_k^f$ is the same as single femtocell beamforming method explained in the previous section and its formulation is shown below.

$$\boldsymbol{V}_k^f = \boldsymbol{h}_k^{fm} \tag{4.27}$$

When the beamforming method is applied to two FAP, the size of $\boldsymbol{V}_k^f$ changes. Three base stations, one MBS and two FAP, are involved in beamforming process. Formulation is as follows.

$$\boldsymbol{V}_k^f = [\boldsymbol{h}_k^{fm}, \boldsymbol{h}_{k,j}^{ff}] \tag{4.28}$$

4.2.2. Simulation Results

In multiple FAP scheme, beamforming method is implemented depending upon the amount of power received from each FAP on MUE. This scheme is also divided into two different situations. First, the FAP which has the greatest interference power on MUE is chosen as the one which is applied beamforming method. Thus, one FAP is used in implementing the process. After the FAP to be used is selected, the applied beamforming technique is same as the single femtocell case in previous sections. In this scenario, MBS has four antennas while FAPs have two antennas. Secondly, beamforming is applied to two of four femtocells which have the greatest interference powers on MUE and this represents the second situation in multiple FAP scheme. Here, since there are three base stations to be applied beamforming, the antenna number of FAPs is assumed to be three.

In the given scenario for multiple FAP environment, the results of this technique are shown based on SINR values of individual user by using graphs and images. It is assumed that the transmit power of FAP is 23 dBm and that of MBS is 43 dBm.

The following figure, Figure 4.8, shows detailed information about how the SINR of MUE changes with respect to the location or, in other words, distance to the individual FAP and whether the FAP to which beamforming is implemented is accurately chosen. Three figures are seen in that figure. The first sub-figure, on the top of Figure 4.8, illustrates FAPs layout in which MUE moves toward to the determined-direction in order to show where the MUE is. The third sub-figure, undermost of Figure 4.8, indicates which FAP is chosen at a given particular location of MUE in order that beamforming is implemented. In here, index 1 indicates the first FAP to be chosen while index 2 indicates second one. Index 2 is only used in beamforming schemes with two FAPs. The second sub-figure, in the middle of Figure 4.8, represents the core figure. It shows the SINR changing and gives a comparable sight of SINR plottings among two situations in the beamforming method and without beamforming method.

It can be clearly seen that Figure 4.9 is in the same format with Figure 4.8. The only difference is that the MUE has different route for each of them. In Figure 4.9, MUE is moving from FAP3, whose coordinate is (600,800), to FAP 2 along the diagonal whereas MUE, in Figure 4.8, is moving from FAP1 to the FAP4. In both figures, x-axes of graphs represent dfm, distance from FAP to MUE. In Figure 4.8, dfm denotes the distance from FAP1 to MUE while denoting the distance from FAP3 to MUE in Figure 4.9.

As seen in Figures 4.8-4.9, there are great degradations of MUE's SINR when getting closer to the FAPs without using beamforming method. This effect is completely removed when beamforming is applied. Of two beamforming scenarios, as observed, the SINR values of beamforming with two FAPs has better results than the other scenario. As for choosing the FAP to be beamformed, the algorithm is successfully implemented since indexing responds accurately to the changes in the MUE location.

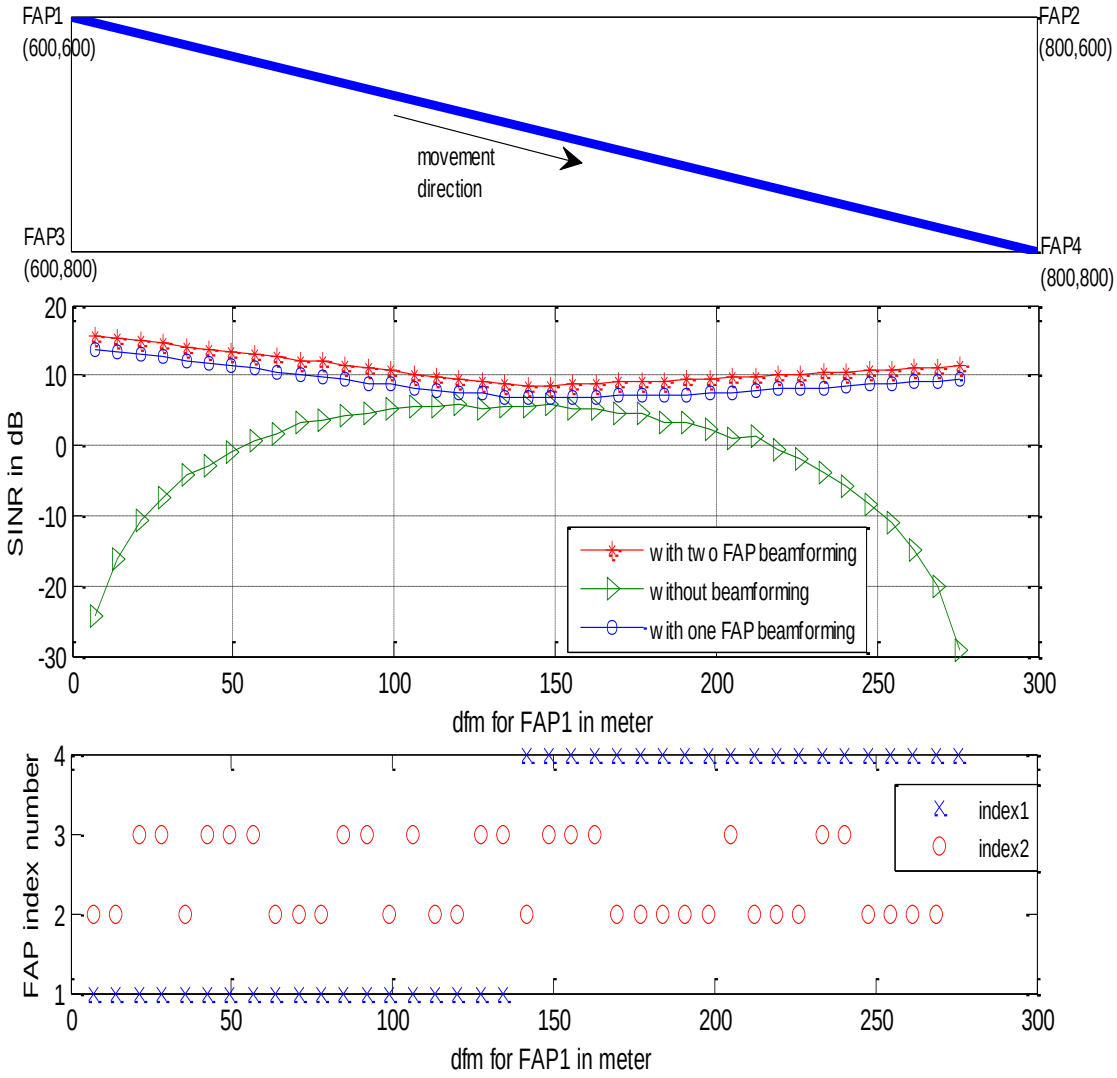

Figure 4.8. SINR of MUE moving from FAP1 to FAP4 and indexing FAP

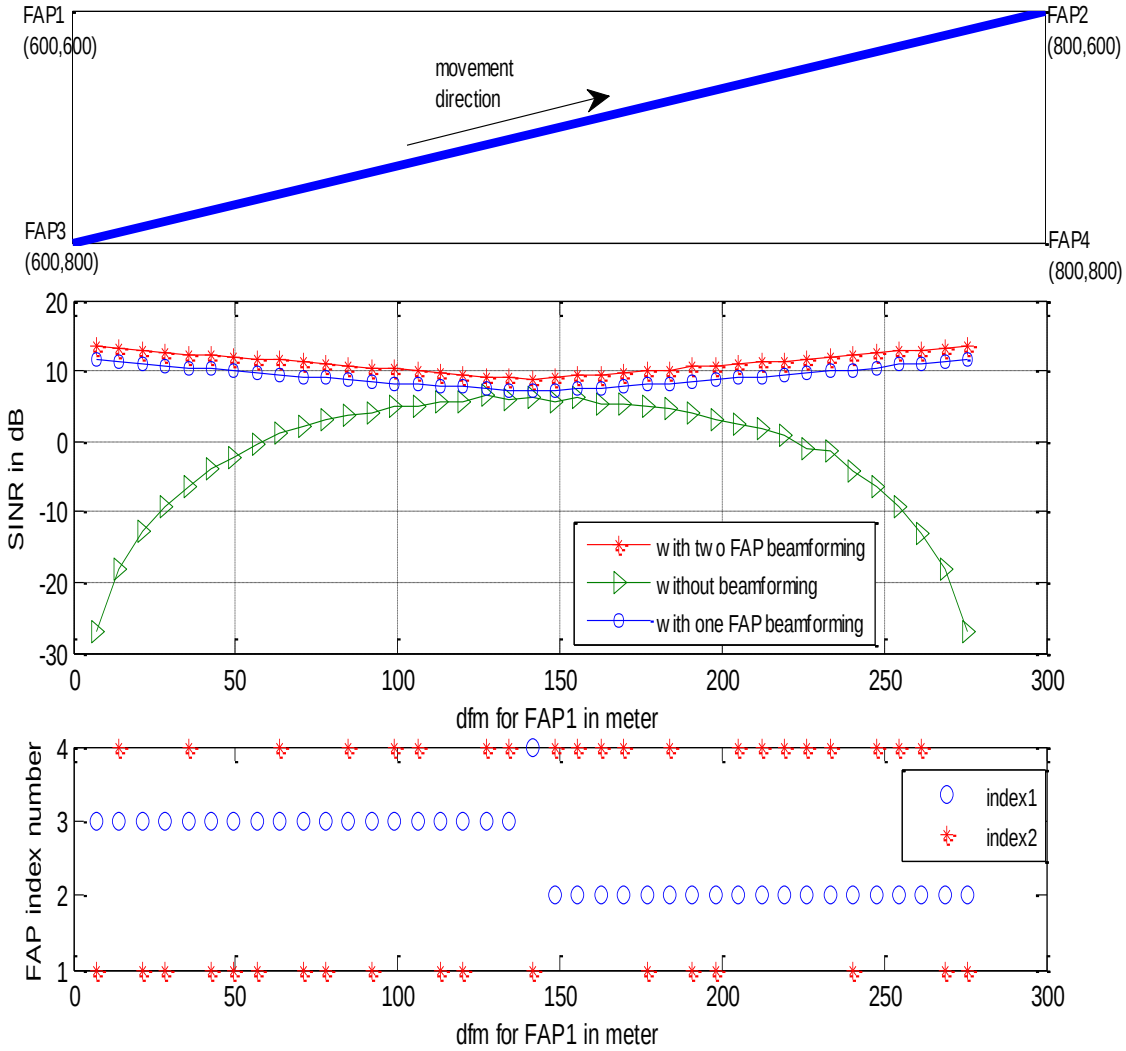

Figure 4.9. SINR of MUE moving from FAP3 to FAP2 and indexing FAP

CHAPTER 5

JOINT POWER CONTROL AND BEAMFORMING TECHNIQUE

In wireless systems, methods which is applied for better system performance should not only works perfectly but also make the most of efficiency in present situation. Aforementioned power control technique works well but deadzone phenomenon imposes large burden on MUE in some cases. Additionally, beamforming technique completely suppresses cross-tier interference to be sure. However, FAP and MBS use its maximum available transmit power, which brings about transmit power consumption to a large degree.

Taking into account this fact, the idea that beamforming and power control technique are considered as jointly would be better. The aim here is that total transmission power consumed by femto base stations is minimized while maintaining the SINRs of all users in the system above a minimum target value. In this way, interference problem can be resolved by minimum transmit power.

This chapter deals with the joint technique in two cases. First, the technique applied to the system with one FAP is explained. Then, the technique in multiple FAP environment is explained. Simulation results of each individual case are evaluted.

5.1. Joint Power Control and Beamforming Technique in Single Femtocell

5.1.1. System Model

In this work, power control and beamforming with partial zero forcing techniques are implemented jointly. System model given in Figure 3.1 is used as a basis for this technique. In here, two differrent formulations of each technique regarding to power control and beamforming technique are just combined. General formulation of the proposed joint technique is as follows.

$$\min_{w}(P^{tf}) \tag{5.1}$$

subject to

$$\gamma^{m} \geq \gamma^{mtar} \tag{5.2}$$

$$\gamma^{f} \geq \gamma^{ftar} \tag{5.3}$$

where γ^{mtar} and γ^{ftar} are the target SINR for the MUE and FUE, respectively. The received SINRs γ^{m} and γ^{f} are described as in Equations (4.1) and (4.2). The channel gains are also the same as the beamforming technique, which are written in Equations from (4.3) to (4.6).

5.1.1.1. The Proposed Joint Algorithm for Single FAP

Firstly, in order to avoid cross-tier interference effect, channel vectors are eliminated by designing beamforming weight vectors which are orthogonal to them. In addition, the weight vectors are delivered to maximize co-layer channel vectors as well.

Secondly, based on these weight vectors, SINR values are formed with respect to the Equations (4.1) and (4.2). These SINRs, when substituted into Equations (5.2) and (5.3), give maximum and minimum transmission power range of femtocell, as follows.

$$P^{tf} \leq \left[\frac{P^{tm}G^{mm}}{PL^{mm}\,N^{tm}\,\gamma^{mtar}} - N_0 B\right] PL^{fm}N^{tf} \Big/ G^{fm} \tag{5.4}$$

$$P^{tf} \geq \left[\frac{P^{tm}G^{mf}}{PL^{mf}N^{tm}} + N_0 B\right] \gamma^{ftar}\; PL^{ff}N^{tf} \Big/ G^{ff} \tag{5.5}$$

Of these two equations, Equation (5.5) enables femtocell transmission power to be minimized in a way that targeted SINR values can be achieved at the same time.

As a result, power control problem allows femtocell to make the most of its power efficiency while beamforming weight vectors cancel the interference effects

coming from cross-layers of network. In this way, both cross-tier interference cancellation and transmission power minimization are carried out by means of joint technique.

5.1.2. Simulation Results

Joint power control and beamforming technique is of great use to the systems which are aiming at both interference-free environment and power-efficient base stations. To show the effects of this technique, results which are obtained from the Equations (5.4) and (5.5) are illustrated in this section. Simulation parameters are taken from Table 3.1.

In order to observe how the interference effect is suppressed, Figure 5.1 is shown in following page. SINR of MUE is stabilized even though MUE is so close to the nearby FAP. In that figure, MUE's trajectory is also shown in order to provide good understanding of plotting under study. dfm in the x-axis, distance between FAP and MUE, increases in compliance with the trajectory of MUE. As seen, SINR does not undergoes any degradation with the help of used joint technique. From this aspect, so-called figure proves the joint tecnique to be so effective in cancelling cross-tier interference.

In order to observe how the energy-efficiency is achieved, Figure 5.2 can be given as an example. This figure has a comparison between power control and joint technique. It goes to show that the tranmission power of femtocell, when the joint technique is used, can be reduced to a large degree. In so-called figure, femtocell power changes with respect to the distance of FUE to the femtocell due to the controllable-nature of it. From this respect, it has the same characteristics with the power control technique. However, the difference of transmission powers between two technique is more or less 20 dB. Joint technique has a clear advantage over the power control technique alone in respect of power consumption.

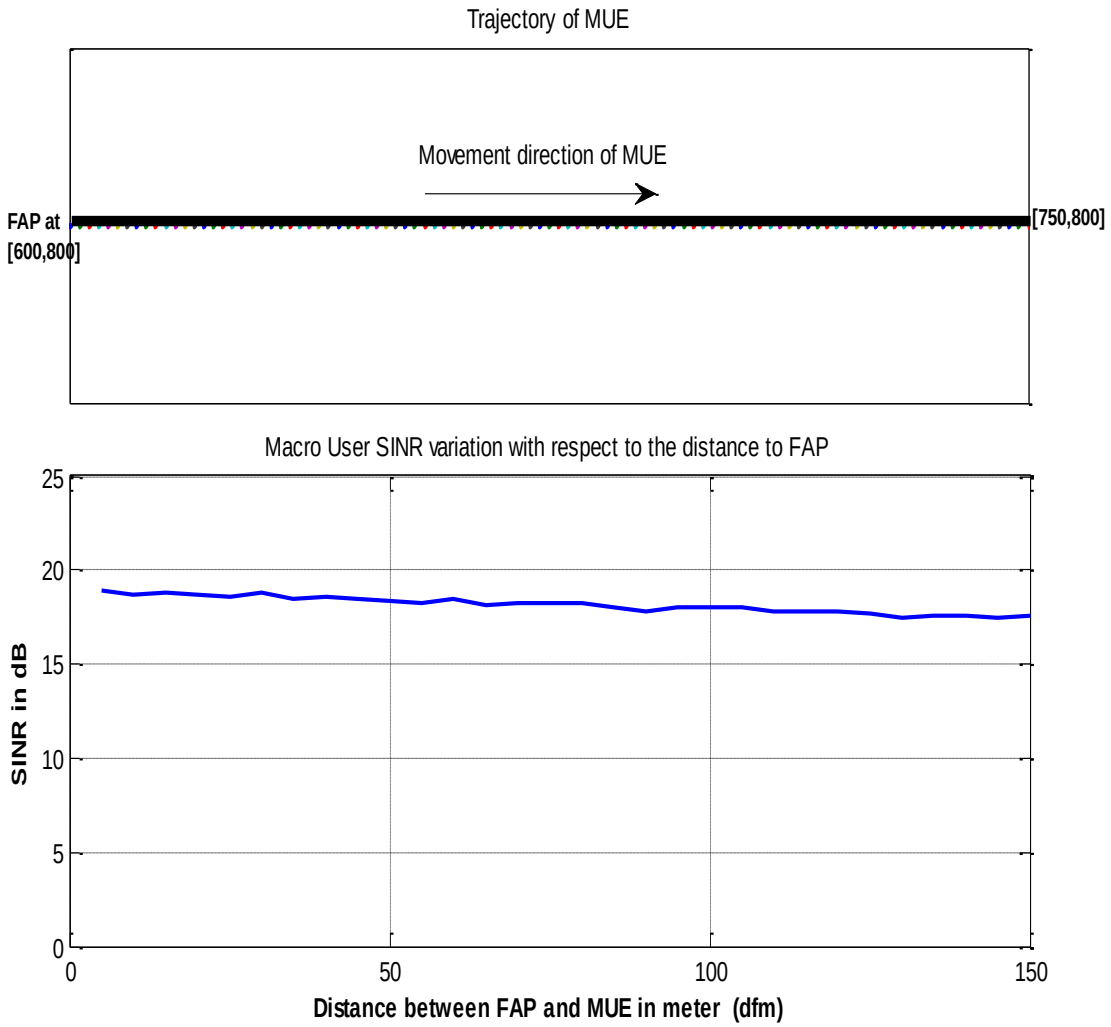

Figure 5.1. SINR of MUE vs distance between FAP and MUE

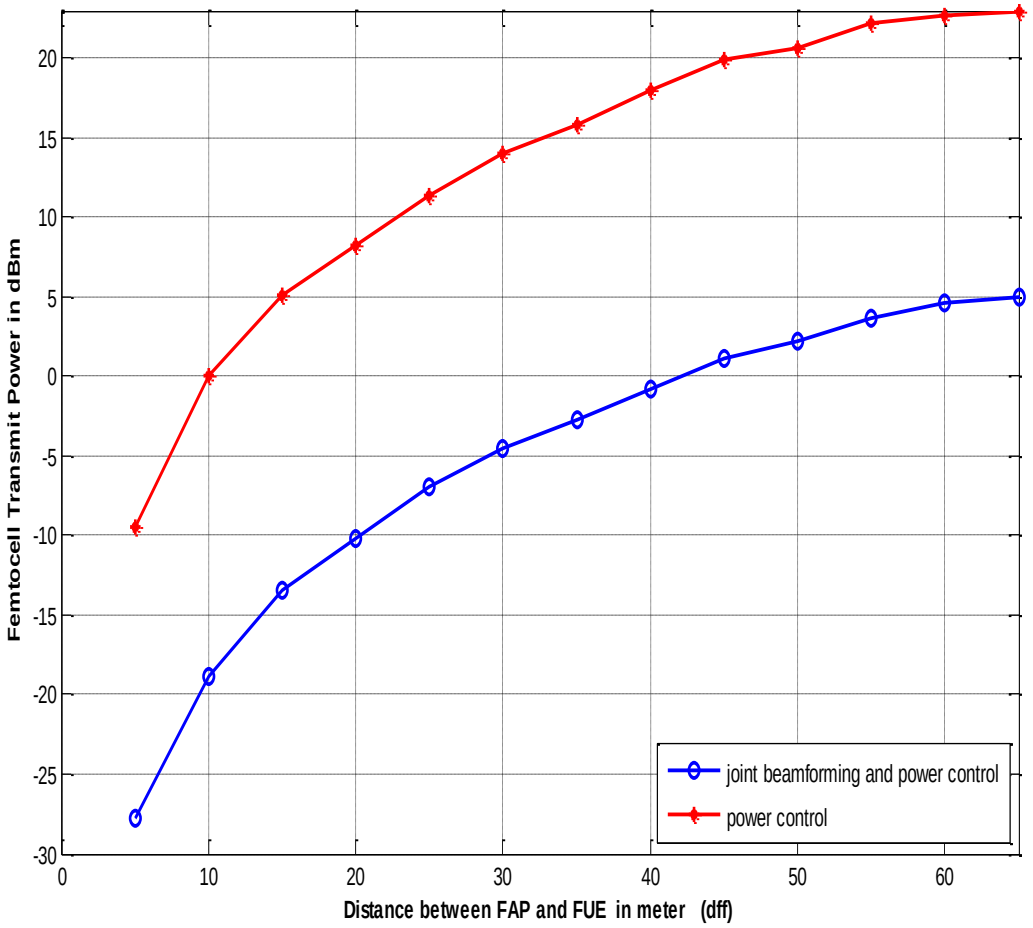

Figure 5.2. Comparison of the joint technique with power control technique

5.2. Joint Power Control and Beamforming Technique in Multiple Femtocells

In multiple FAPs configuration, system performance can be boosted by applying joint technique. Given the benefits of joint technique in the single FAP case, power efficiency issues are of far more importance when it comes to multiple FAP system. Besides, interference suppression can be handled. This section is intended for showing that how the joint technique works and responds, when applied to the multiple FAPs.

Considering the whole system established in this work, the concerned method is thought as a joint technique but the power control and beamforming techniques are implemented individually to all FAPs. First, FAP which has the greatest interference power on MUE is selected to apply beamforming technique in order to cancel this interference power and then, power control technique is applied to the rest of the FAPs in area. Thus, both interference cancellation and power efficiency issues are ensured as a whole.

5.2.1. System Model

The system model shown in Figure 3.7 is taken as a basis for multi FAP system under study. In this work, beamforming and power control techniques are applied to the FAPs in order to suppress the cross-tier interference on MUE which is coming from FAPs and to enable FAPs to adjust their powers in a more effective manner while satisfying their users (FUEs).

5.2.1.1. The Proposed Joint Algorithm for Multiple FAPs

Problem formulization is divided into two parts. The first part is concerned with beamforming technique and the second one deals with power control technique. Beamforming technique is applied to one of the four FAPs which has the greatest interference power on MUE. This is determined by measuring all the received powers on MUE at a given location. In order to produce beamforming vectors for chosen FAP whose index is k and for MBS, the following vectors are written down as

$$\boldsymbol{V}_k^f = \boldsymbol{h}_k^{fm} \tag{5.6}$$

$$\boldsymbol{V}^m = \boldsymbol{h}_k^{mf} \tag{5.7}$$

where $\boldsymbol{h}_k^{fm}$ is channel vector between k^{th} FAP and MUE, and also $\boldsymbol{h}_k^{mf}$ is the channel vector between MBS and k^{th} FUE. $\boldsymbol{V}_k^f$ is a vector with the size of 2×1 and $\boldsymbol{V}^m$ is a vector with the size of 4×1. Then, the beamforming vectors are determined by

$$\boldsymbol{w}_k^f = (\boldsymbol{I} - \boldsymbol{Z}_k^f)\boldsymbol{h}_{k,k}^{ff} \tag{5.8}$$

$$\boldsymbol{w}^m = (\boldsymbol{I} - \boldsymbol{Z}^m)\boldsymbol{h}^{mm} \tag{5.9}$$

where the projection matrix on $\boldsymbol{V}_k^f$ and $\boldsymbol{V}^m$ are as follows

$$\boldsymbol{Z}_k^f = \boldsymbol{V}_k^f((\boldsymbol{V}_k^f)^H\boldsymbol{V}_k^f)^{-1}(\boldsymbol{V}_k^f)^H \tag{5.10}$$

$$\boldsymbol{Z}^m = \boldsymbol{V}^m((\boldsymbol{V}^m)^H\boldsymbol{V}^m)^{-1}(\boldsymbol{V}^m)^H \tag{5.11}$$

In this way, beamforming vectors, $\boldsymbol{w}^m$ and $\boldsymbol{w}_k^f$, are produced in the direction of the projection of the channel vectors, $\boldsymbol{h}_{k,k}^{ff}$ and $\boldsymbol{h}^{mm}$, and orthogonality criterion, $\boldsymbol{w}_k^f\boldsymbol{h}_k^{fm} = 0$ and $\boldsymbol{w}^m\boldsymbol{h}_k^{mf} = 0$, is achieved. Thus, cross-tier interference issue is handled with the help of this criterion. In order to see the effects of these criterions on the SINR parameters, below-mentioned equations can be followed. Firstly, channel gains are

$$G^{mm} = \left|(\boldsymbol{h}^{mm})^H\ \boldsymbol{w}^m\right|^2 \tag{5.12}$$

$$G_k^{mf} = \left|(\boldsymbol{h}_k^{mf})^H\boldsymbol{w}^m\right|^2 \tag{5.13}$$

$$G_{k,k}^{ff} = \left|(\boldsymbol{h}_{k,k}^{ff})^H\boldsymbol{w}_k^f\right|^2 \tag{5.14}$$

$$G_k^{fm} = \left|(\boldsymbol{h}_k^{fm})^H\boldsymbol{w}_k^f\right|^2 \tag{5.15}$$

where G^{mm} is channel gain between MBS and MUE, G_k^{fm} is channel gain between k^{th} FAP and MUE, $G_{k,k}^{ff}$ is the one between k^{th} FAP and k^{th} FUE, G_k^{mf} is the one between

MBS and k^{th} FUE. These gains ultimately take place in the SINR formulations of MUE and FUE, as follows.

$$\gamma^m = \frac{(P^{tm} / PL^{mm} N^{tm}) G^{mm}}{\sum_k (P_k^f G_k^{fm} / PL_k^{fm} N^{tf}) + N_0 B} \tag{5.16}$$

$$\gamma_k^f = \frac{(P_k^{tf} / PL_{k,k}^{ff} N^{tf}) G_{k,k}^{ff}}{(P^{tm} / PL_k^{mf} N^{tm}) G_k^{mf} + N_0 B} \tag{5.17}$$

After the beamforming process is implemented to one chosen FAP with index k by means of abovementioned formulas, power control method is conducted among the rest of the FAPs whose indexes are denoted by " j ". In power control technique, the main aim is to provide power efficiency for base stations making sure that users achieve satisfying SINR values. For this reason, formulization is based on the target SINR values of users, as follows.

$$\gamma^m \geq \gamma^{mtar} \tag{5.18}$$

$$\gamma_j^f \geq \gamma_j^{ftar} \tag{5.19}$$

$$P^{f\min} \leq P_j^{tf} \leq P^{f\max} \tag{5.20}$$

where γ^{mtar} and γ^{ftar} are the target SINR for the MUE and FUE, respectively. $P^{f\min}$ and $P^{f\max}$ are the minimum and maximum allowable transmission power of the FAP. j is the index of FAPs remaining from beamformed FAP. γ^m and γ_j^f is written for power control technique as below.

$$\gamma^m = \frac{P^{tm} / PL^{mm}}{\sum_j (P_j^{tf} / PL_j^{fm}) + N_0 B} \tag{5.21}$$

$$\gamma_j^f = \frac{P_j^{tf} / PL_{j,j}^{ff}}{P^{tm} / PL_j^{mf} + N_0 B} \tag{5.22}$$

These SINR equations, when substituted into Equations (5.18) and (5.19), enable maximum and minimum FAP power bounds to be founded as follows.

$$P^{f\max} \leq \left[\frac{P^{tm}}{PL^{mm} \quad \gamma^{mtar}} - N_0 B \right] \tag{5.23}$$

$$P_j^{f\min} \geq \left[\frac{P^{tm}}{PL_j^{mf}} + N_0 B \right] \gamma^{ftar} \; PL_{j,j}^{ff} \tag{5.24}$$

Here, $P_j^{f\min}$ is the minimum power of FAP to satisfy its own user. $P^{f\max}$ is the maximum FAPs power gathered on MUE, which indicates the maximum allowable interference power onto MUE and is formulated as

$$P^{f\max} = \sum_j (P_j^f / PL_j^{fm}) \qquad j = 1,...,4 \text{ and } j \neq k \tag{5.25}$$

This equation shows that transmission powers of each FAP in the area except for k^{th} FAP are all summed up to find a maximum interference power limit. In order to determine in which way each individual FAP adjusts its power so that FAPs cannot pose an interference to the MUE, based on Equation (5.25) above, the total power, $P^{f\max}$, can be shared among FAPs in a distance-based manner. In order to do this, the coefficient is produced by dividing total received power to the sum of distances from all the FAPs to the MUE, as follows.

$$coef = P^{f\max} \Big/ \sum_j dfm_j \tag{5.26}$$

This coefficient is used in sharing the total power between femtocells with the help of the formula shown below.

$$p_j^f = coef \; dfm_j \tag{5.27}$$

$$P_j^{f\max} = p_j^f \; PL_j^{fm} \tag{5.28}$$

Thus, by using $P_j^{f\max}$ and $P_j^{f\min}$, feasible transmission power of FUEs is obtained and power control tehnique is formed. As a result, having looked at the whole system from the multi-cell perspective, the so-called technique can be regarded as a joint.

5.2.2. Simulation Results

In multi FAP system model, there are four femtocell access point. Here, beamforming technique is applied to one chosen FAP which has the greatest interference power on MUE while power control technique is applied to the rest of FAPs. This provides both interference suppression and power efficiency at same time. These advantageous capabilities show itself in the simulation results with the help of graphs in the following pages. In the power control technique, the target SINR values for MUE and FUE are taken as 10 dB.

Figure 5.3 shows detailed information about how the SINR of MUE changes with respect to the location and has a comparison between joint and beamforming techniques. Three figures are seen in that figure. The first sub-figure, on the top of Figure 5.3, illustrates FAPs layout in which MUE moves toward to the determined-direction in order to show where the MUE is. The third sub-figure, undermost of Figure 5.3, indicates which FAP is chosen at a given particular location of MUE in order that beamforming is implemented The second sub-figure, in the middle of Figure 5.3, shows the SINR changing and gives a comparable sight of SINR plottings between two techniques. As seen in this figure, MUE, when being close to FAPs, do not undergoes any degradation effects, which proves joint technique to suppress the cross-tier interference. Furthermore, a small amount of decreasing in SINRs of MUE results from the fact that MUE is moving away from MBS as seen in the trajectory graph.

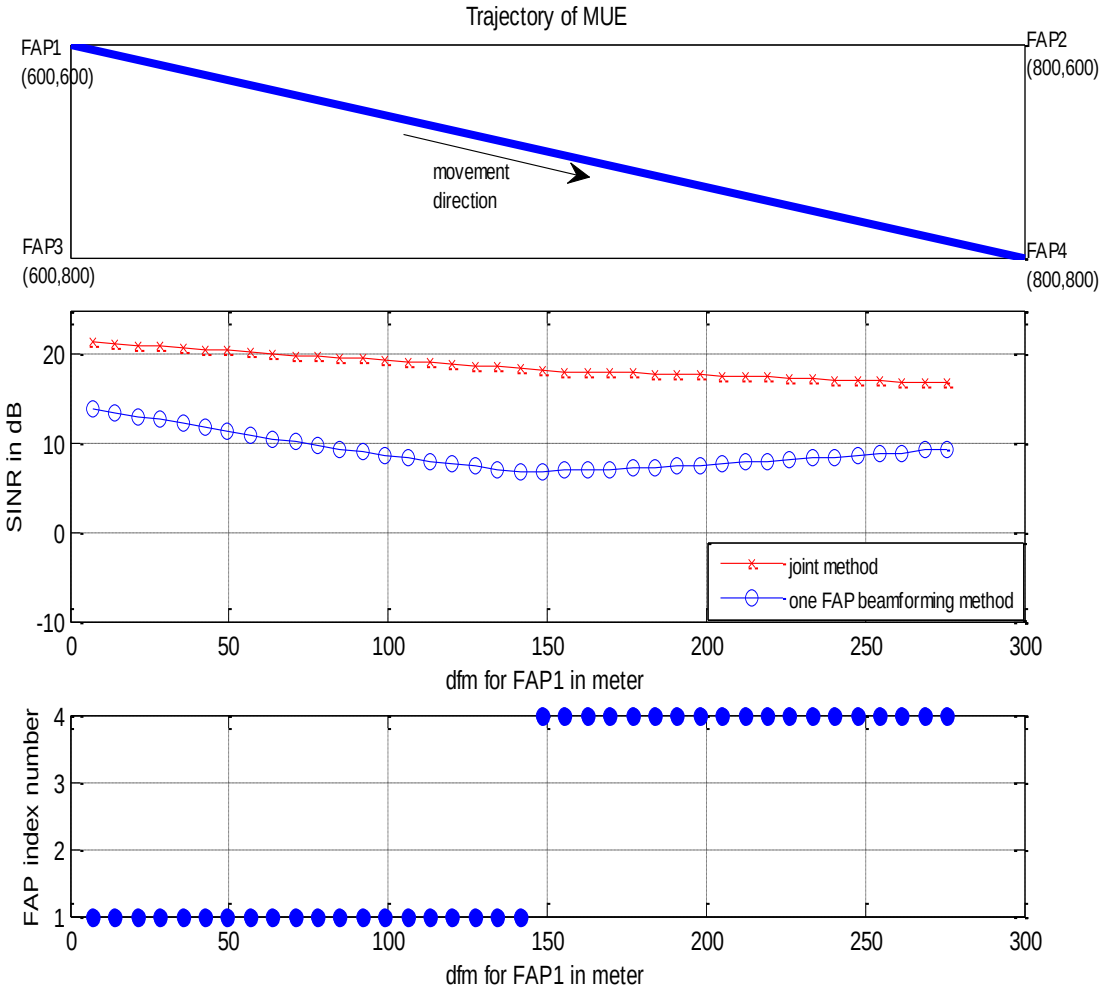

Figure 5.3. SINR of MUE moving from FAP 1 to FAP 4 and indexing number of beamformed FAP in joint method

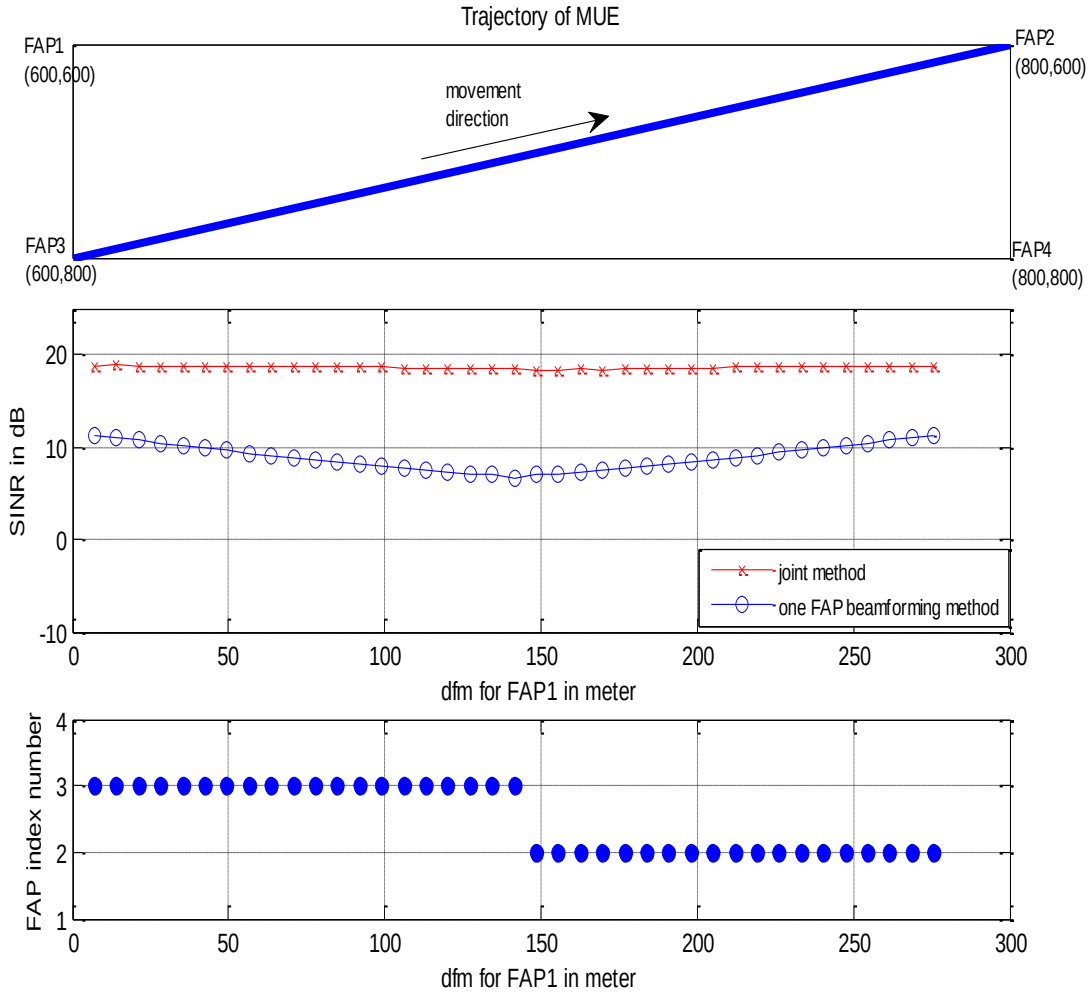

Figure 5.4. SINR of MUE moving from FAP 3 to FAP 2 and indexing number of beamformed FAP in joint method

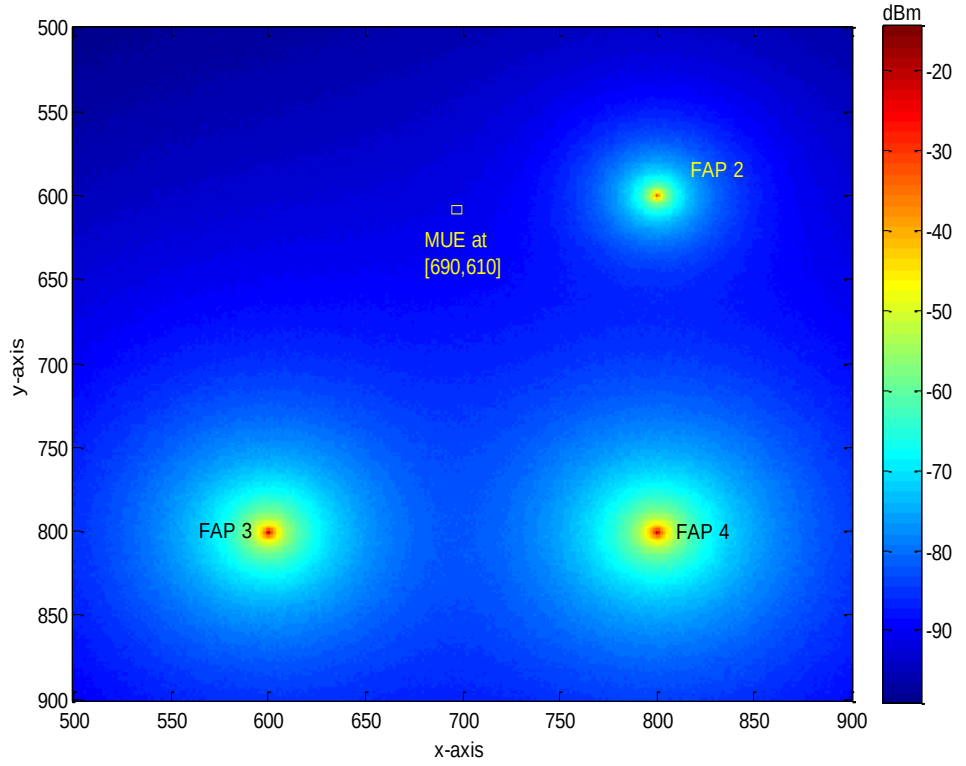

Figure 5.5. Power distribution of FAPs with MUE at (690,610)

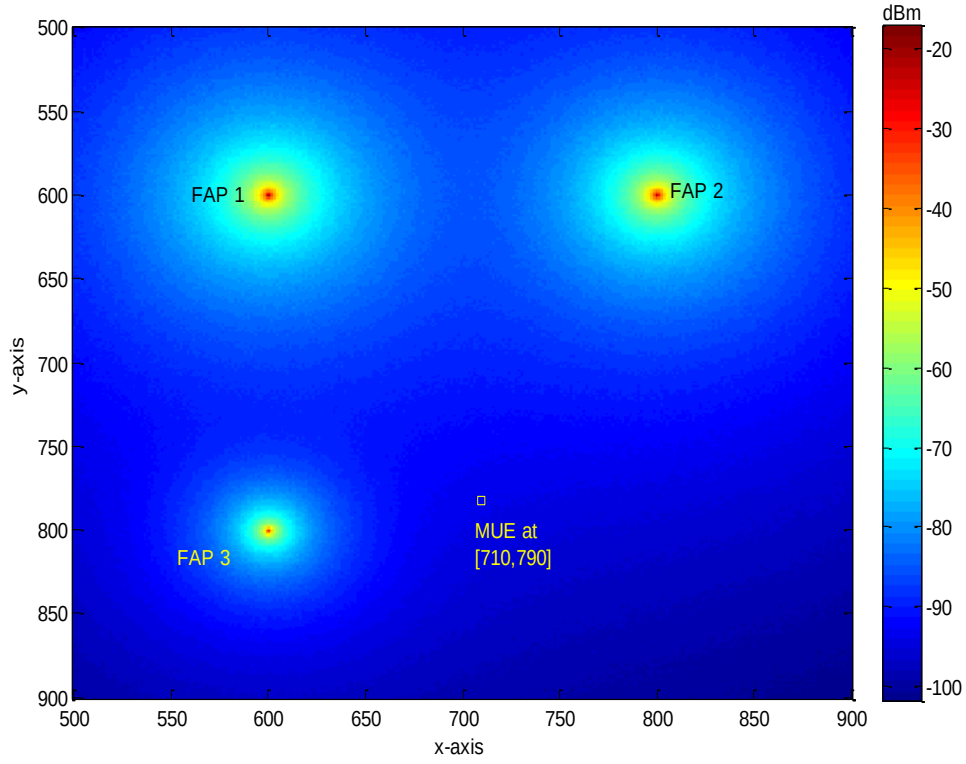

Figure 5.6. Power distribution of FAPs with MUE at (710,790)

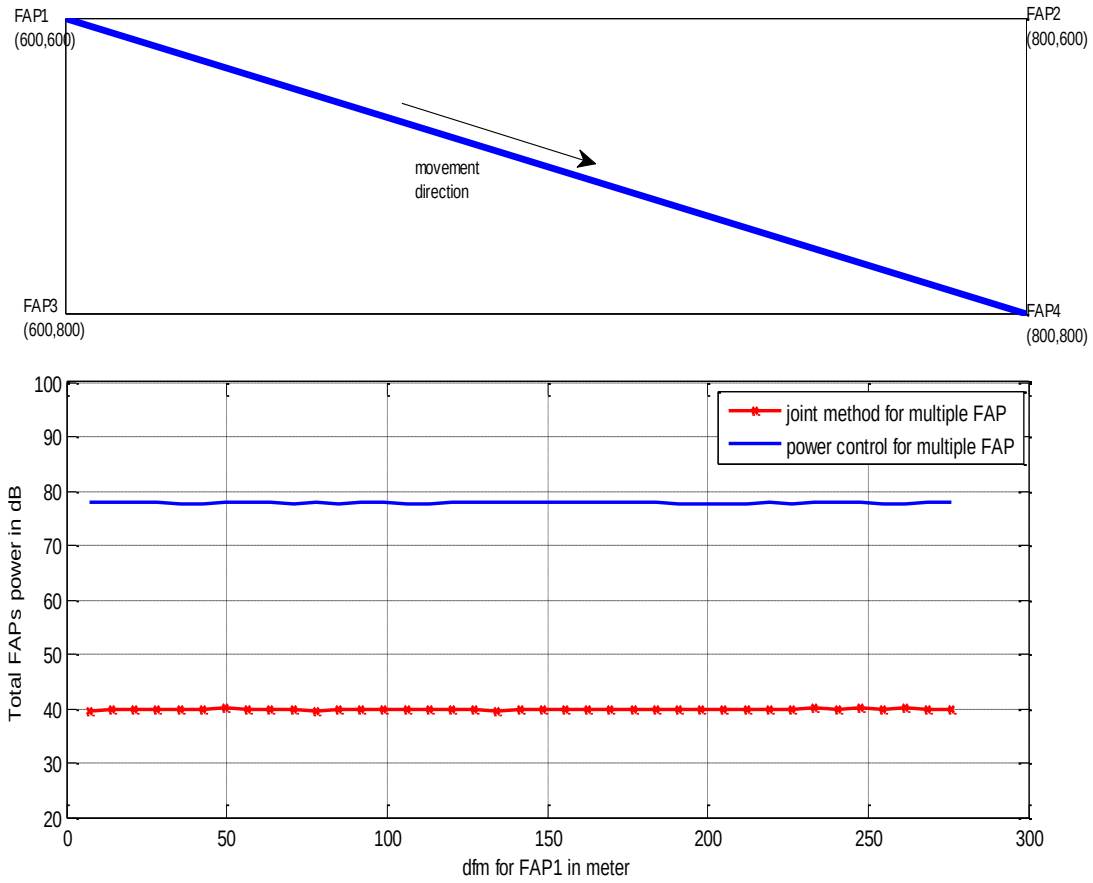

Figure 5.7. Total power consumption for femtocells

Figure 5.4 serves for the same way as Figure 5.3 does. However, MUE moves over the different path compares to Figure 5.3. In Figure 5.4, MUE is moving from FAP3, whose coordinate is (600,800), to FAP 2 along the diagonal whereas MUE, in Figure 5.3, is moving from FAP1 to the FAP4. In both figures, x-axes of graphs represent dfm, distance from FAP to MUE. In Figure 5.3, dfm denotes the distance from FAP1 to MUE while denoting the distance from FAP3 to MUE in Figure 5.4.

In addition to the beamforming technique, illustrating the power distribution of the FAP in area, Figures 5.5 and 5.6 show how the power control works and which FAP is chosen to apply beamforming method. In these figures, the powers of FAPs which are selected for beamforming process are not shown because they have no effects on MUE. In Figure 5.5, MUE is located at the coordinates of (690,610). Here, FAP 1 is selected for beamforming method because it has a strongest interference power in this case. As seen, FAP 2 has a lowest power because of its close-range to MUE. Since the distances of the other FAPs are approximately the same, there is no observable difference between their powers. Moreover, Figure 5.6 is the counterpart of the previous figure. MUE is located at (710,790). Here, FAP 4 is selected for beamforming process. Considering the distances of each FAP to the MUE, power sharing or controlling is successfully achieved for FAPs as seen in Figure 5.6.

In order to see how the joint technique achieves power-efficiency for femtocells, Figure 5.7 can be given as an example. This figure consists of trajectory of MUE and summation of transmit powers of FAPs in area with respect to the distance dfm. It is clearly seen that total consumed FAP power, when joint technique is employed, far less than that of the power control method for multiple FAP. Joint technique is much more power-efficient technique compared to power control.

CHAPTER 6

CONCLUSION

In this thesis, interference management techniques have been studied for two-tier network which is made up of femtocell and macrocell layers. Two techniques, in particular, have been dealt with jointly and separately. These are power control and beamforming techniques. These techniques have been examined in the two distinct system models. One of these models consists of single FAP and single MBS while the other is made up of multiple FAPs and single MBS.

Power control problem, first, has investigated in a system model with one MBS and FAP which each of them has one user. Then, the so-called technique has applied to a multiple FAPs system. The problem has been simply formulated in a way that femtocell adjusts its power depending on the distances of macro and femto users in order to maintain SINR values. At the same time, macrocell user nearby FAP has been prevented from interference signal coming from femtocell by decreasing transmission power of the FAP. The effects of this power control on FAP is clearly observed in power distributions of FAPs in the multiple FAPs case. All in all, feasible transmit power region for all the FAPs is obtained. This means that SINRs of all users in femtocell coverage area is satisfied with the help of power control method. However, in the event that MUE is closer to the nearby FAP than FUE, it has been observed that power control technique does not work properly and deadzones have come into being for MUE in the region at issue. From this perspective, power control technique needs much research to be done.

Secondly, beamforming technique has been implemented to cancel cross-tier interference by employing partial zero-forcing method. In this method, interference which belong to the different tiers are suppressed by beamforming weight vectors which are designed to provide orthogonality. With that, interference signals coming from nearby base stations have been able to be cancelled and cross-tier interference has been removed. This technique has been implemented for both single and multiple FAPs cases. In single FAP case, when beamforming is employed, there has been no degradation in SINR values of MUE which is in the vicinity of FAP. It has been also

observed that SINR of FUE is improved with this method. In multiple FAPs case, beamforming method has been applied to one FAP which has the strongest interference power on MUE and two FAPs which have the strongest interference power on MUE. In either case, it is observed that interference on MUE has been removed. Also, from the comparative SINR graphs of MUE it follows that beamforming with two FAPs is slightly better than beamforming with one FAP.

Finally, power control and beamforming techniques have been jointly applied. In single FAP case of this technique, beamforming weight vectors make it possible for interference signal to be cancelled while power control enables FAP to select minimum transmission power. As a result of this, it has been shown that these two technique, when applied jointly, not only provide cross-tier intereference suppression but also enable femtocell to consume less power than ever before. Thus, joint technique proves to be power-efficient interference management solution when compared to individual techniques. In multiple FAP case, the joint technique has been applied differently. In here, beamforming method has been applied to one FAP which has the strongest interference power on MUE and, power control has been performed for all the other FAPs in the system. The proposed technique works properly in terms of avoiding interference over MUE and controlling powers of FAPs.

For future femtocell networks, there is no doubt that interference management will eventually become the major concern because of, likely, dense deployment of FAPs. The imperfect channel state information can be considered for joint power control and beamforming technique for femtocell networks.

REFERENCES

[1] V. Chandrasekhar and J. Andrews, "Femtocell networks: A survey", *IEEE Commun. Mag. , vol. 46, no. 9, pp. 59–67, Sep. 2008.*

[2] N. Saquib, E. Hossain, L. Le Bao, D. I. Kim, " Interference Management in OFDMA Femtocell Networks : Issues and Approaches ", *IEEE Wireless Communications, pp. 86-95, June 2012.*

[3] G. Mansfield, "Femtocells in the US Market –Business Drivers and Consumer Propositions", *FemtoCells Europe, ATT, London, U.K. , June 2008.*

[4] M. Yavuz, F. Meshkati, S. Nanda, A. Pokhariyal, N. Johnson, B. Roghothaman, and A. Richardson, "Interference management and performance analysis of umts/hspa+ femtocells", *IEEE Commun. Mag. , vol. 47, no. 9, pp. 102–109, Sep. 2009.*

[5] H. Daehyoung, C. Seungwoong, and C. Jaeweon, "Coverage and capacity analysis for the multi layer cdma macro/indoor picocells", *IEEE International Conference on Communications, vol. 1, pp. 354–358, 1999.*

[6] H. Yankikomeroglu and E. S. Sousa, "Power control and number of antenna elements in cdma distributed antenna systems", *IEEE International Conference on Communications, vol. 2, pp. 1040–1045, 7-11 Jun 1998.*

[7] T. Zahir, K. Arshad, A. Nakata, K. Moessner, " Interference Management in Femtocell ", *IEEE Communications Surveys & Tutorials, Vol. 15, pp. 293-311, First Quarter 2013.*

[8] Stallings W. , 2005. "Wireless Communications and Networks", *Upper Saddle River, NJ: Prentice Hall.*

[9] Goldsmith A. , 2005. " Wireless Communications " , *Cambridge University Press.*

[10] "Universal Mobile Telecommunications System (UMTS), Selection Procedures for the choice of radio transmission technologies of the UMTS (UMTS 30.03 version 3.1.0)", *European Telecommunications Standards Institute (ETSI), 1997.*

[11] J. Mietzner, R. Schober, L. Lampe, W.H. Gerstacker, P.A. Hoeher , " Multiple-Antenna Techniques for Wireless Communications – A Comprehensive Literature Survey " , *IEEE Communications Surveys & Tutorials, Vol. 11, No. 2, pp. 87-105, Second Quarter 2009.*

[12] D. Chambers, “Femtocell history”, *online available at: http://www.thinkfemtocell.com/FAQs/femtocell-history.html.*

[13] H. Claussen, “Performance of macro and co channel femtocells in a hierarchical cell structure ”, *IEEE 18th International Symposium on Personal, Indoor and Mobile Radio Communications, pp. 1–5, 3-7 September 2007.*

[14] M. Fan, M. Yavuz, S. Nanda, Y. Tokgoz, and F. Meshkati, “Interference management in femto cell deployment ”, *in 3GPP2 Femto Workshop, October 2007.*

[15] J. O. Carroll, H. Claussen, and L. Doyle, “Partial GSM spectrum reuse for femtocells ”, *IEEE 20th International Symposium on Personal, Indoor and Mobile Radio Communications, pp. 2111–2116, 13-16 September 2009.*

[16] S. S. Prasad and R. Baruah, “Femtocell mass deployment: Indian perspective ”, *3rd International Conference on Anti-counterfeiting, Security, and Identification in Communication, pp. 34–37, 20-22 August 2009.*

[17] M. Neruda, J. Vrana, and R. Bestak, “Femtocells in 3G mobile networks ”, *16th International Conference on Systems, Signals and Image Processing, pp. 1–4, 18-20 June 2009.*

[18] D. Knisely, T. Yoshizawa, and F. Favichia, “Standardization of femtocells in 3GPP ”, *IEEE Commun. Mag. , vol. 47, no. 9, pp. 68–75, September 2009.*

[19] L. Wang, Z. Yongsheng, and W. Zhenrong, “Mobility management schemes at radio network layer for lte femtocells ”, *IEEE 69th Vehicular Technology Conference, pp. 1–5, 26-29 April 2009.*

[20] R. Y. Kim, S. K. Jin, and K. Etemad, “WiMAX femtocell: requirements, challenges, and solutions ”, *IEEE Commun. Mag. , vol. 47, no. 9, pp. 84–91, September 2009.*

[21] D. Lopez-Perez, A. Valcarce, G. de la Roche, J. Zhang, “ OFDMA Femtocells : A Roadmap on Interference Avoidance ”, *IEEE Communication Magazine, pp. 41-48, September 2009.*

[22] J. Zhang, G. de la Roche, E. Liu, 2010. “ Femtocells: Technologies and Deployment ”, *John Wiley and Sons Ltd., pp. 1-13.*

[23] S. F. Hasan, N. H. Siddique, and S. Chakraborty, “Femtocell versus Wi Fi- A survey and comparison of architecture and performance ”, *1st International*

Conference on Wireless Communication, Vehicular Technology, Information Theory and Aerospace and Electronic Systems Technology, pp. 916–920, 17-20 May 2009.

[24] J. L. V. D. Berg, R. Litjens, A. Eisenbltter, M. Amirijoo, O. Linnell, C. Blondia, T. Krner, N. Scully, J. Oszmianski, and L. C. Schmelz, "Self-organisation in future mobile communication networks ", *ICT - Mobile Summit, Sweden, vol. 2, pp. 915–920, June 2008.*

[25] J. S. Young, G. H. Hae, and K. S. Kwang, "A self organised femtocell for ieee 802.16e system ", *IEEE Global Telecommunications Conference, pp. 1–5, November 30-December 4 2009.*

[26] S.A. Khwandah, J.P. Cosmas, " Interference Management in LTE Co-channel Femtocells ", *Broadband Multimedia Systems and Broadcasting (BMSB), IEEE International Symposium, pp. 1-5, 25-27 June 2014.*

[27] L. Yang, S.H. Song, K.B. Letaief, " Cognitive Spectrum Access in Two-Tier Femtocell Networks ", *ICC – IEEE International Conference, Sydney, pp. 5354-5359, 10-14 June 2014.*

[28] D. Chen, T. Jiang, Z. Zhang, " Frequency Partitioning Methods to Mitigate Cross-tier Interference in Two-tier Femtocell Networks ", *IEEE Transactions on Vehicular Technology, Issue 99, pp. 1-12, July 2014.*

[29] T. Mao, G. Feng, L. Liang, S. Qin, B. Wu, "Distributed Energy-Efficient Power Control for Macro-Femto Networks ", *IEEE Transactions on Vehicular Technology, pp. 1-13, February 2015.*

[30] I. Ahmad, Z. Feng, A. Hameed, P. Zhang, Y. Zhao, "Spectrum Sharing and Energy-Efficient Power Optimization for Two-tier Femtocell Networks ", *9th International Conference on Cognitive Radio Oriented Wireless Networks and Communications (CROWNCOM), Oulu, pp. 156-161, 2-4 June 2014.*

[31] S. He, L. Zhang, X. Wen, Z. Zhang, Z. Lu, Y. Sun, " Price-based Power Control with Statistical Delay QoS Guarantee in Two-tier Femtocell Networks ", *21st International Conference on Telecommunications (ICT), Lisbon, pp. 318-322, 4-7 May 2014.*

[32] C.C. Tseng, C.S. Peng, S.H. Lo, H.C. Wang, F.C. Kuo, K.C. Ting, " Co-tier Uplink Power Control in Femtocell Networks by Stackelberg Game with Pricing ", *4th International Conference on Wireless Communications, Vehicular Technology, Information Theory and Aerospace & Electronic Systems (VITAE), Aalborg, pp. 1-5, 11-14 May 2014.*

[33] H.O. Kpojime, G.A. Safdar, " Interference Mitigation in Cognitive Radio based Femtocells ", *IEEE Communications Surveys and Tutorials, pp.1-72, October 2014.*

[34] M. Chiang, P. Hande, T. Lan, C.W. Tan, 2008. " Power Control in Wireless Cellular Networks ", *Foundation and Trends in Networking Sample, pp. 21-47*.

[35] M. S. Jin, S. Chae, and D. I. Kim, "Per Cluster Based Opportunistic Power Control for Heterogeneous Networks ", *Proc. IEEE VTC'11 Spring, Budapest, Hungary, May 2011*.

[36] X. Li, L. Qian, D. Kataria, " Downlink Power Control in Co-Channel Macrocell Femtocell Overlay ", *43rd Annual Conference on Information Sciences and Systems, Baltimore, pp. 383-388, 18-20 March 2009.*

[37] Y. Jeong, Tony Q.S. Quek, H. Shin, " Beamforming Optimization for Multiuser Two-Tier Networks ", *KICS Journal of Communications and Networks, vol. 13, no. 4, pp. 327-338, August 2011*.

[38] F. Rashid-Farrokhi, K. J. R. Liu, L. Tassiulas, " Transmit Beamforming and Power Control for Cellular Wireless Systems ", *IEEE Journal on Selected Areas in Communications, Vol. 16, No. 8, pp. 1437-1450, October 1998.*

[39] N.Jindal, J.G. Andrews, S. Weber, " Rethinking MIMO for Wireless Networks : Linear Throughput Increases with Multiple Receive Antennas ", IEEE International Conference on Communications (ICC), Dresden, Germany, 2009.